POLITECNICO DI MILANO

Dipartimento di Elettronica, Informazione e Bioingegneria

COMPARATIVE ANALYSIS OF MODELS FOR THE ASSESSMENT OF TIBIOFEMORAL CONTACT LOADS DURING CYCLING AND GAIT TRIALS

Relatore: Prof.ssa Manuela Galli

Correlatore: Prof. Stephen Klisch

Tesi di laurea di:

Alberto Palumbieri Matr. 876549

Anno accademico 2018/2019

Acknowledgment

I would like to thank all the people who contributed in some way to the work described in this thesis. First and foremost, I thank Professor Stephen Klisch for accepting me into his group, in Human Motion Biomechanics (HMB) lab at California polytechnic state university.
During my stay, he contributed to a rewarding graduate school experience by giving me intellectual freedom in my work, supporting my attendance at various meetings, engaging me in new ideas, and demanding a high quality of work in all my endeavors.
Additionally, I would like to thank all the HMB lab staff and Prof. Scott Hazelwood for their help and interest in my work.
Every result described in this thesis was accomplished with the help and support of fellow labmates and collaborators among which I want to say a special thanks to Shaida Biglari, she was an extremely reliable source of practical scientific knowledge and I am very grateful for all her support.
Then, I want to thank prof. Alberto Redaelli and my thesis advisor prof. Manuela Galli for their effort, allowing me to get in contact with prof. Klisch and spend 6 months at California Polytechnic state university.
Furthermore, since with this work my university course in coming to an end, I want to say thanks to everyone has been close to me all these years long. My family, especially my parents, that believed in me more than I did for all these years. My friends, especially Oswaldo and Kevin, which have been great study partners as well.

Abstract

Model selection is one of the most important modeling choices in the OpenSim environment. Many models have been developed over the years with varying degrees of accuracy and intended use. Analyzing knee joint contact loads provides insight into the knee loading conditions which are strongly related to diseases such as knee osteoarthritis. Unphysiological tibiofemoral compartment loads are related to pathologic conditions, therefore nowadays is very important to exploit models able to provide medial and lateral knee contact load components. The two most used OpenSim models to date have been presented by Zach Lerner [17] and by Adrian Lai and Allison Arnold [18].

Zach Lerner created a model able to split the TibioFemoral (TF) contact loads into medial and lateral components, the drawback of this kind of model is that is not accurate for high knee flexion angles, while the model presented by Lai can overcome Lerner drawback but doesn't show any knee loads partition. Since it hasn't been provided so far, this study aims to offer a comparison among these two models to understand which can be the best operations to merge these two models. Other aim of this study is to prove the bounty of the ML tibiofemoral load partitioning proposed by Lerner [17], which is hypothesized with ML loads equally shared among the two compartments during cycling, while with a heavier medial engagement during gait. [25, 26]

To reach these goals 5 participants performing gait and cycling tasks have been tested through a motion analysis system (Motion Analysis Corp. Santa Rosa, CA, USA) with 12 digital cameras recording motion and 4 force plates (Accugait, AMTI, Watertown, MA, USA) recording ground reaction forces.

The provided data were already processed in Cortex. The data processing has been performed following the OpenSim workflow, consisting in Scale tool, inverse kinematics analysis, residual reduction algorithm, static optimization, joint reaction analysis and inverse dynamics analysis. The tibiofemoral contact forces have been obtained from joint reaction analysis while knee flexion/extension and abduction/adduction moments have been obtained from inverse dynamics. These parameters underwent to a MATLAB interpolation and to an average on 3 trials for each participant, both for gait and cycling.

A statistical comparison exploiting Minitab paired t-test has been performed, based on flexion/extension moment, abduction/adduction moment and tibial contact force in their maximal, minimal and average values, and Mediolateral tibiofemoral Force Ratio (MLFR) in its maximal value.

The results show that maximum MLFR ($p < 0,05$) is significantly different for gait compared to cycling, with gait showing maximum medial contact force 4 times higher than cycling, while cycling presents a more equal distribution of the force, matching the hypothesis made for this parameter.

The maximum, minimum and average TF contact force ($p < 0,01$) during cycling is significantly different for Lerner [17] compared to Lai [18]. This discrepancy has been explained looking at the muscle force produced in the high knee flexion angle range, which shows that the muscle parameters set in Lai [18] bring to an higher muscle force prediction.

Important considerations have been made on the complexity of the two models, dealing with the opportunity to choose the right model in which transfer the main features of the compared one. Lerner presents a higher number of bodies and muscles with respect to Lai which could be hard to transfer. Lai shows the same problem regarding its wrapping surfaces, introduced to improve the simulation speed, that aren’t present in Lerner model and could be computationally hard to transfer.

Sommario

La selezione del modello è una delle scelte più importanti nell'ambiente OpenSim.
Molti modelli sono stati sviluppati nel corso degli anni con vari gradi di precisione e diversa destinazione d'uso. L'analisi dei carichi di contatto dell'articolazione del ginocchio fornisce informazioni dettagliate sulle condizioni di carico di tale articolazione che sono fortemente correlate a malattie come l'artrosi del ginocchio. I carichi non fisiologici del compartimento TibioFemorale (TF) sono correlati a condizioni patologiche, pertanto oggigiorno è molto importante sfruttare modelli in grado di predire le componenti di carico di contatto mediale e laterale del ginocchio. I due modelli OpenSim più utilizzati fino ad oggi sono quelli presentati da Zach Lerner [17] e da Adrian Lai insieme ad Allison Arnold [18].
Zach Lerner ha creato un modello in grado di suddividere il carico di contatto tibiofemorale nelle componenti mediale e laterale, lo svantaggio di questo tipo di modello è che non è preciso per angoli di flessione del ginocchio elevati. D'altro canto, sebbene il modello presentato da Lai possa superare i problemi di approccio di Lerner ad angoli di flessione del ginocchio elevati, sfortunatamente non mostra alcuna partizione dei carichi tibiofemorali.
Dal momento che non è stato ancora eseguito, questo studio mira a offrire un confronto tra questi due modelli per capire quali possono essere le operazioni migliori per effettuarne la fusione delle caratteristiche principali.
Altro scopo di questo studio è dimostrare la bontà del partizionamento del carico tibiofemorale MedioLaterale (ML) proposto da Lerner [17], che è ipotizzato con carichi ML equamente ripartiti tra i due scomparti durante le prove di pedalata, mentre è previsto con un maggiore impegno mediale durante le prove di camminata. [25, 26]
Per raggiungere questi obiettivi sono stati testati 5 partecipanti che hanno eseguito prove di pedalata e cammino attraverso un sistema di analisi del movimento (Motion Analysis Corp. Santa Rosa, California, USA) con 12 videocamere digitali che hanno registrato il movimento e 4 piastre di forza (Accugait, AMTI, Watertown, MA, USA) per la rilevazione delle forze di reazione al suolo.
I dati forniti erano già stati elaborati in Cortex. La successiva elaborazione dei dati è stata eseguita seguendo il flusso di lavoro di OpenSim, costituito da strumento di scalatura, analisi cinematica inversa, algoritmo di riduzione dei residui, ottimizzazione statica, analisi delle reazioni articolari e analisi della dinamica inversa.
Le forze di contatto tibiofemorale sono state ottenute dall'analisi delle reazioni articolari mentre i momenti di flessione / estensione del ginocchio e di abduzione / adduzione sono stati ottenuti

dall’analisi della dinamica inversa. Questi parametri sono stati interpolati in MATLAB e mediati su 3 prove per ciascun partecipante, sia per le prove di cammino che di pedalata.

È stato eseguito un confronto statistico in Minitab attraverso t-test, in cui sono stati analizzati momento di flessione/estensione, momento di abduzione/adduzione e forza di contatto tibiofemorale nei loro valori massimi, minimi e medi ed inoltre è stato analizzato il rapporto di forza tibiofemorale medio-laterale (MLFR) nel suo valore massimo.

I risultati mostrano che il MLFR massimo ($p < 0,05$) è significativamente diverso per la camminata rispetto alla pedalata, la prova di cammino mostra la massima forza di contatto mediale 4 volte superiore rispetto alla pedalata, mentre la prova di pedalata presenta una distribuzione più equa della forza. Il parametro MLFR si mantiene quindi aderente alle ipotesi iniziali in entrambi i casi.

La forza di contatto TF massima, minima e media ($p < 0,01$) durante la pedalata è significativamente diversa per Lerner [17] rispetto a Lai [18]. Questa discrepanza è stata spiegata osservando la forza muscolare prodotta nel range di elevata flessione del ginocchio, portando a dimostrare che i parametri muscolari impostati in Lai [18] portano a una predizione della forza muscolare più elevata.

Importanti considerazioni sono state fatte sulla complessità dei due modelli, affrontando il tema dell'opportunità di scegliere il modello giusto in cui trasferire le caratteristiche principali dell’altro modello confrontato.
Lerner presenta un numero maggiore di corpi (bodies) e muscoli rispetto a Lai che potrebbero essere difficili da trasferire. Lai mostra lo stesso problema per quanto riguarda le sue superfici di avvolgimento, introdotte per migliorare la velocità di simulazione, che non sono presenti nel modello di Lerner e potrebbero essere difficili da trasferire a livello computazionale.

List of figures

List of equations

List of tables

Table of contents

CHAPTER 1

INTRODUCTION

The knee experiences relatively high biomechanical loads during activities of daily living. Walking, for example, induces knee contact forces as large as three times bodyweight at the knee [1]. Joint loads affect the development, maintenance, and health of the joint tissues [2]. The onset and progression of diseases such as knee osteoarthritis have been linked to abnormal biomechanical loads [3], and increased knee loads have been linked to pain severity in patients with osteoarthritis [4].

Improve injury-prevention exercise guidelines for populations that are at high risk for knee osteoarthritis requires to understand the degeneration of biological knee joints, this can be done due to the knowledge of the in-vivo loading environment during activities of daily living. Musculoskeletal models can estimate tibiofemoral (TF) contact forces, yet anthropometric differences between individuals make accurate predictions challenging.

Experimental evidence points out the trend that non-impact exercises, such as cycling, have lower tibiofemoral (TF) loads than high impact exercises such as gait or running on knee health [5], [6]. However, the loads present at the TF joint are multi-dimensional due to the complex muscle structure in the thigh and shank that transmit forces to and across the joint. In general, there are 3 forces (compressive, anterior-posterior (AP) shear, and medial-lateral (ML) shear) and 3 rotation moments (flexion-extension, varus-valgus, and internal-external) being applied.

Additionally, the contact geometry of the TF joint is a function of the flexion angle. Therefore, while the compressive force may be different in one exercise compared to another, the addition of shear forces and rotation moments compounded by the changing joint angle means that understanding the relationship between exercise type and the contact pressure is not trivial. Determination of these relationships is a goal of OpenSim simulation.

It is worth to perform an assessment of the existing OpenSim models to understand which can be the development of the next updates in this field. This study aims to provide valid information to merge Lerner [17] and Lai models [18].

Create a model showing the best characteristics of the two mentioned precursors can lead towards a more accurate TF load prediction both for gait and cycling without the necessity of changing the model. Furthermore, this solution can help people approaching musculoskeletal dynamic simulations to save up a lot of time. For example, the scaling process in OpenSim is a time-consuming task that allows the creation of a subject-specific simulation. To get accurate simulation results, the generic model must be “scaled” to better match the real participant. This is achieved by a slow and frustrating task, consisting in moving virtual markers on the generic model to locations better representing the positions of the actual markers placed on the participant. Dispose of two different models for gait and cycling means the necessity of using the scale tool two times, avoid this work surplus can only be beneficial.

1.1 OpenSim models

An OpenSim model represents the neuromuscular and musculoskeletal dynamics of a human or animal that is of interest to study within a computer simulation. The OpenSim model is made up of components corresponding to parts of the physical system that combine to generate or describe movement. These parts are reference frames, bodies, joints, constraints, forces, contact geometry, markers and controllers. In OpenSim, a model's skeletal system is represented by rigid bodies interconnected by joints. Joints define how two bodies (e.g., bone segment), termed parent and child bodies, can move with respect to one another. Constraints can also be applied to limit the motion of bodies. Muscles are modeled as specialized force elements that act at muscle points (e.g., insertion and origin points) connected to rigid bodies.

The force of a muscle is typically dependent on the path through muscle points comprised of muscle fiber and tendon lengths, the rate of change of the fiber lengths, and the level of muscle activation. OpenSim also has a variety of other forces, which represent externally applied forces (e.g., ground reaction forces), passive spring-dampers (e.g., ligaments), and controlled linear and torsional actuators [38].

The figure 1.1 shows a conceptual schematic of an OpenSim model. In the remainder of the paragraph, the OpenSim model file format used to describe these models is discussed. These properties can be edited using scripts, via an XML editor.

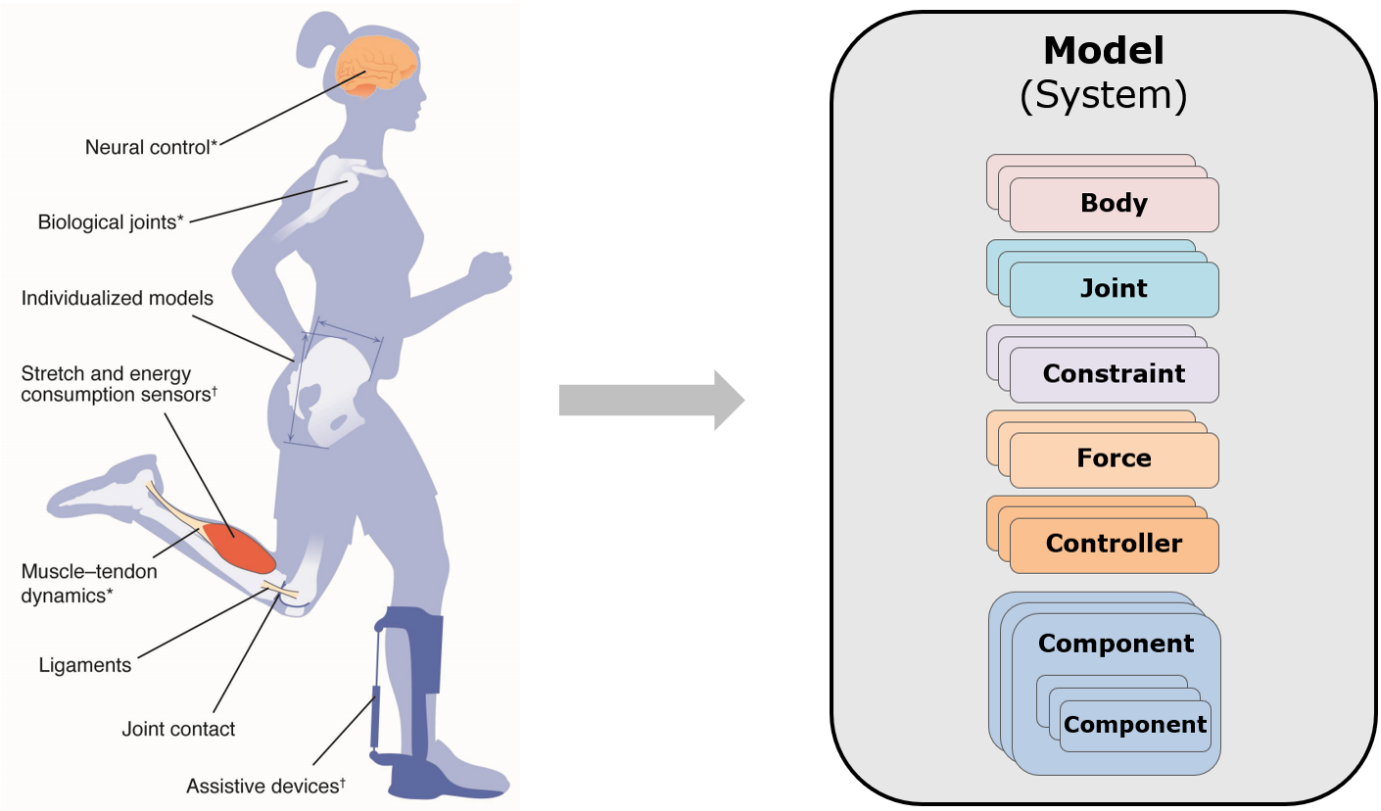

Figure 1.1. Conceptual schematic of an OpenSim model.

An OpenSim model is described by a file that utilizes the XML code structure to organize its contents. XML uses tags to identify and manage information, such as:

```
<gravity>0 -9.8065999999999995 0</gravity>
```

where **<gravity>** signifies the opening of the tag, **0 -9.8065999999999995 0** is a vector describing the acceleration due to gravity, and **</gravity>** signifies the end of the tag. The name of the tag identifies the type of information between the tags. When editing an OpenSim model file, there are tags representing each part of the model, as shown in the figure 1.2.

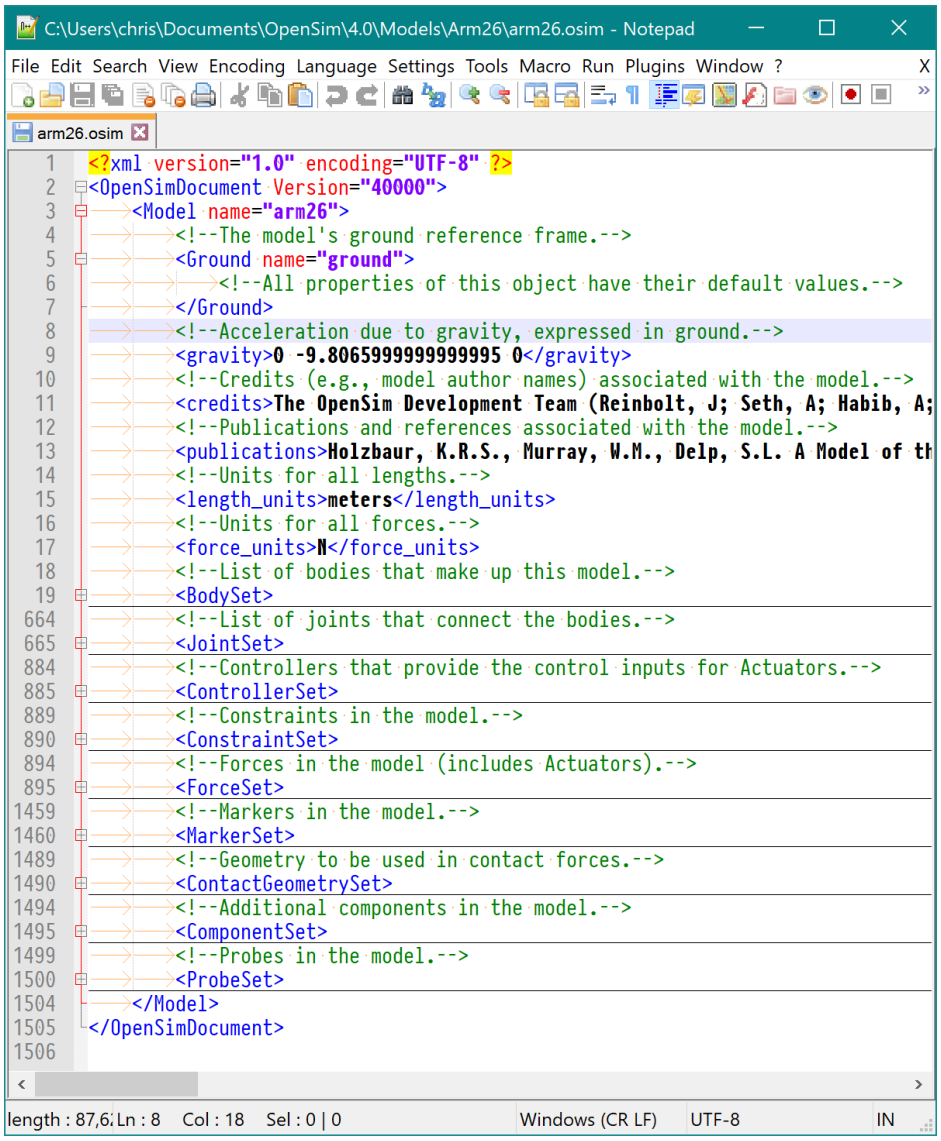

Figure 1.2. OpenSim model code.

It is common for components to depend on each other. For example, Joint components depend on the Body components (actually, PhysicalFrames) that the Joint connects.

To specify these dependencies, OpenSim uses the notion of Sockets. As you will see later, a Joint has two Sockets: **parent_frame** and **child_frame**. You can specify the frames that satisfy these sockets in XML:

<socket_parent_frame>/ground</socket_parent_frame>

<socket_child_frame>/bodyset/r_humerus</socket_child_frame>

Any XML element whose tag begins with **socket_** is used to indicate the path to a component (ComponentPath) in the model that should be used to satisfy the socket.

Models in OpenSim are hierarchical, this means that components can contain other components. For example, the BodySet component named 'bodyset' contains the Body component 'r_humerus'. Forward slashes are used, similar to a file system path or web URL, to indicate the path to a component in the model's hierarchy. In the example above, absolute paths starting with a slash have been used, but relative paths (e.g., ../../some/other/component) also work.

In formulating the equations-of-motion (i.e., the system dynamics), OpenSim employs Simbody which is an open-source multibody dynamics solver. In Simbody and OpenSim, the body is the primary building block of the model. Each body in turn owns a joint that connects it to an existing parent body. The joint defines the coordinates and kinematic transforms that govern the motion of that body with respect to its parent body. Within the model all bodies are contained in a BodySet. Thus, to start the model, is worth to define a set of rigid bodies that represent the system. In the **<BodySet>** section, this group of bodies are defined, with the name, mass properties, and visible objects associated with each body.
Regarding the body geometry there isn't the necessity to specify a mesh file to use most analytical shapes (Brick, Sphere, Cylinder, Cone, Ellipsoid). In addition, can be specified Mesh to indicate geometry read from a mesh file. It is possible to use .vtp, .stl, or .obj files to visualize geometry. All these types are kinds of Geometry.

Additionally, to the set of rigid bodies, we also need to define the relationship between those bodies (i.e., joint definitions). In the figure below, a joint (in red) defines the kinematic relationship between two frames (B and P) each affixed to a rigid-body (the parent, P_o, and the body being added, B_o) parameterized by joint coordinates

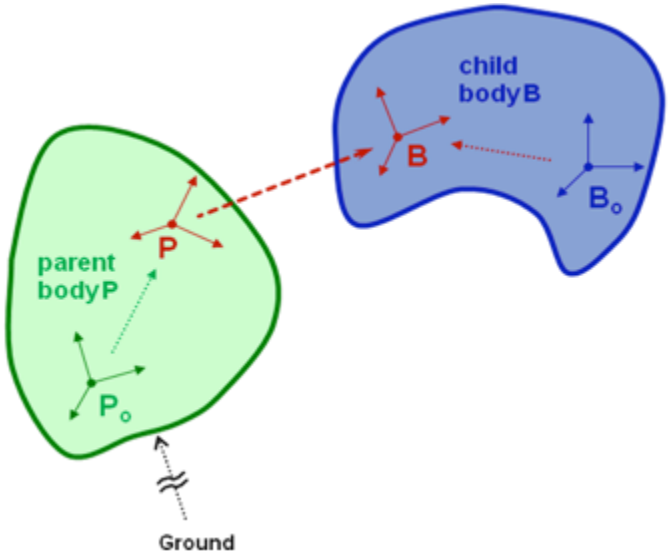

Figure 1.3. kinematic relationship between two frames (B and P) affixed to rigid-bodies.

A body is a moving reference frame (B_o) in which its center-of-mass and inertia are defined, and the location of a joint frame (B) fixed to the body can be specified. Similarly, the joint frame (P) in the parent body frame (P_o) can also be specified. Flexibility in specifying the joint is achieved by permitting joint frames that are not coincident with the body frame. This flexibility is enhanced via the introduction of the **Frame** class hierarchy. There are three main types of Frames: **Ground** (each model starts with a ground frame), **Body**, and **PhysicalOffsetFrame**. All three of these frames are called **PhysicalFrames** because they either are a rigid body or are fixed to a rigid body, a joint connects two **PhysicalFrames** (parent and child). One can use **PhysicalOffsetFrames** to specify a constant transform between a joint frame and the body frame.
Among the available joint types can be found:

- WeldJoint: introduces no coordinates (degrees of freedom) and fuses bodies together.
- PinJoint: one coordinate about the common Z-axis of parent and child joint frames.
- SliderJoint: one coordinate along common X-axis of parent and child joint frames.
- BallJoint: three rotational coordinates that are about X, Y, Z of B in P.
- EllipsoidJoint: three rotational coordinates that are about X, Y, Z of B in P with coupled translations such that B traces and ellipsoid centered at P.
- FreeJoint: six coordinates with 3 rotational (like the ball) and 3 translations of B in P.
- CustomJoint: user specified 1-6 coordinates and user defined spatial transform to locate B with respect to P.

Most joints in an OpenSim model are custom joints since this is the most generic joint representation, which can be used to model both conventional (pins, slider, universal, etc.) as well as more complex biomechanical joints. The user must define the transform (rotation and translation) of the child in the parent (B and P, in the joint definition figure above) as a function of the generalized coordinates listed in the Joint's CoordinateSet. Consider the spatial transform ${}^{P}\mathbf{X}^{B}$:

$$ {}^{P}\mathbf{X}(q)^{B} = \begin{bmatrix} {}^{P}\mathbf{R}^{B}(x_1, x_2, x_3) & \begin{matrix} x_4 \\ x_5 \\ x_6 \end{matrix} \end{bmatrix} \qquad (1.1) $$

Where

$$x(q) = \begin{Bmatrix} f_1(q_1, q_2, \ldots, q_m) \\ f_2(q_1, q_2, \ldots, q_m) \\ \vdots \\ f_6(q_1, q_2, \ldots, q_m) \end{Bmatrix}, \qquad (1.2)$$

q are the joint coordinates, and *x* are the spatial coordinates for the rotations (x_1, x_2, x_3) and translations (x_4, x_5, x_6) along user-defined axes that specify a spatial transform (**X**) according to functions f_i. The behavior of a CustomJoint is specified by its SpatialTransform. A SpatialTransform is comprised of 6 TransformAxis tags (3 rotations and 3 translations) that define the spatial position of B in P as a function of coordinates. Each transform axis enables a function of joint coordinates to operate about or along its axis. The function of *q* is used to determine the displacement for that axis. The order of the spatial transform is fixed with rotations first followed by translations. Subsequently, coupled motion (i.e., describing motion of two degrees of freedom as a function of one coordinate) is easily handled.

Other important feature of OpenSim models is the possibility to define kinematic constraints. OpenSim currently supports three types of built-in constraints: PointConstraint, WeldConstraint, and CoordinateCouplerConstraint. A point constraint fixes a point defined with respect to two bodies (i.e., no relative translations). A weld constraint fixes the relative location and orientation of two bodies (i.e., no translations or rotations). A coordinate coupler relates the generalized coordinate of a given joint (the dependent coordinate) to any other coordinates in the model (independent coordinates). The user must supply a function that returns a dependent value based on independent values.

In order to actuate the model, the forces applied to the model need to be defined. Just like bodies are defined within the **<BodySet>** section, forces are defined in the **<ForceSet>** section of the model file. Forces come in two varieties: *passive* forces like springs, dampers, and contact and *active* forces like springs, idealized linear or torque actuators, and muscles. Active forces that require input (controls) supplied by the user or by a controller are called Actuators and are a subset of the ForceSet.
OpenSim has several built-in forces that include: PrescribedForce, SpringGeneralizedForce, BushingForce, as well as HuntCrossleyForce and ElasticFoundationForce to model forces due to contact, note that contact forces also require defining contact geometry.

OpenSim also includes “ideal” actuators which apply pure forces or torques that are directly proportional to the input control (i.e., excitation) via its optimal force (i.e., a gain). Forces and torques are applied between bodies, while generalized forces are applied along the axis of a generalized coordinate (i.e., a joint axis).

There are several muscle models in OpenSim. All muscles include a set of muscle points where the muscle is connected to bones (bodies) and provide utilities for calculating muscle-actuator lengths and velocities. Internally muscle models may differ in the number and types of parameters. Muscles typically include muscle activation and contraction dynamics and their own states (for example activation and muscle fiber length). The control values are typically bounded excitations (ranging from 0 to 1) which lead to a change in activation and then force. An example of a muscle model is the one described by Thelen [36] and exploited by Lerner [17]. In addition to the muscle properties, its geometry must be defined.

A model may be associated with some specific contact geometry. In OpenSim, contact geometry can be an analytical shape, such as a half-place, sphere, or cube, or a user-defined shape represented in a geometry file**.**

1.2 State of the Art

In this study, the final results have been obtained exploiting OpenSim software, used for dynamic simulations with a human body model. As already mentioned in the previous paragraph OpenSim shows particular features, such as muscle models, that can be called in the XML code representing the model. Furthermore, in the model code can be defined anatomical and functional parameters regarding muscles, tendons etc.

To date, model-based dynamic simulations contribute to the design of a wide range of engineering products and their use is becoming increasingly important in bioengineering as well. In this particular field and research are required models that allow getting useful variables from data obtained through motion analysis experiments.

From these experiments, ground (or pedal) reaction forces and kinematic data can be obtained but then it is worth compute the joints and the muscles contributions. Several kinds of human body models can be built according to the ultimate purpose of this study.

When the aim is to analyze the inter-segmental forces (i.e. the overall generalized forces in the joints) it is sufficient the osteoarticular structure and the calculation of the joint moments and

forces, given the external loads and the motion of the body segments. The inter-segmental forces are composed of the muscular forces, the forces that allow the movement of the joint and the joint reactions or inter-articular forces. To distinguish the muscular forces and the inter-articular forces it is not enough to use an osteoarticular model but is necessary a musculoskeletal model with the different muscles and points of insertion of the tendons. Usually, the only musculoskeletal model is not enough because of the redundancy of the model, then the information about the physiological properties of the muscles are added to have more data. With a series of disorders of the neuromuscular system, it is fundamental to identify these forces because of evaluating treatment or simply to make some considerations about the pathology. Some studies have been conducted using a model to study different pathologies. These diseases include, in general, the disorders about mobility impairments [7] or mobility limitations like cerebral palsy [8, 9], osteoarthritis, osteoporosis and paraplegia [8].

The general idea is to conduct dynamic simulations with a musculoskeletal model that allows the investigation of different movements (ordinary or athletic) and find out the joint loads and the muscle forces. There are now available some software and platforms to develop dynamic simulation of human body movements with musculoskeletal modeling [10, 11]. SIMM (Software for Interactive Musculoskeletal Modeling) was developed in 1994 [12] because of the lack of a standard for representing the models. Before that, researchers needed to develop their software for modeling and dynamic simulations, spending a lot of time and often they didn't provide the implementation to the others [10, 12].

Among the software for dynamic simulations of human motion there are: Anybody (Anybody Technology) [10, 13, 14], Visual 3-D (C-Motion Inc.), or Adams (MSC Software Corp.), the problem is that they don't allow to have a free full access to the source code [10]. Since there was no open-source commercial software, OpenSim (OpenSim, Palo Alto, CA, USA) was developed and introduced at the American Society of Biomechanics Conference in 2007 [10, 15]. This is the software used in this research. The reader can find a more detailed description in Section 2.2.2.

Model selection is one of the most important choices in the OpenSim environment. Many models have been developed over the years with varying degrees of accuracy and intended use.

Among the older OpenSim models developed to measure the changes in total tibiofemoral (TF) contact forces due to variations in muscle activity during walking there's the one of DeMers [16]. This model was limited by the absence of partitioning of the tibiofemoral loads into medial and lateral components. Indeed, some modeling approaches require complex, multi-step analyses, or the use of both full-body gait models and finite element or contact models. Finite element and contact

models rely on an accurate representation of the articulating joint surfaces and require imaging techniques that may be unavailable or prohibitively expensive. Resolving the magnitudes of medial/lateral (ML) forces by approximating ML compartment points of contact is a promising approach for estimating contact forces.

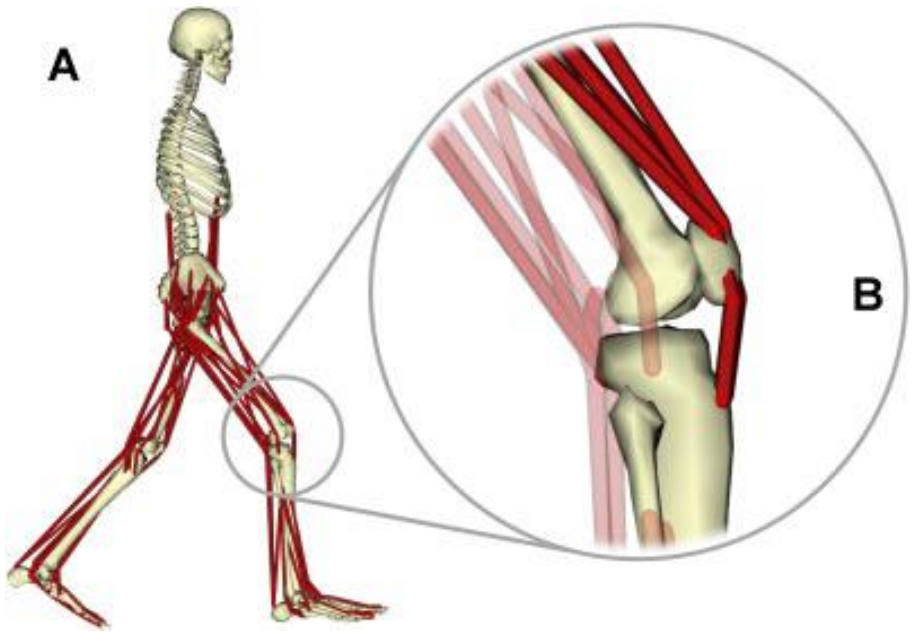

Figure 1.4: *(A) Musculoskeletal model of human leg and torso and (B) expanded details of the tibiofemoral joint used in [5].*

A more recent OpenSim model developed for gait has integrated new structural components into the model of DeMers [16] to partition the total tibial contact force into medial and lateral contact forces, the Lerner model [17]. The distribution of TF contact forces between the ML compartments can be influenced by frontal-plane TF alignment and affect the degeneration of the biological knee [22]. This is why predictions of ML tibiofemoral contact forces in an individual using a musculoskeletal model with generic geometry may be inaccurate when the model does not accurately represent the individual. The specification of certain subject-specific model parameters may improve accuracy [23]. In the model defined by Lerner [17] two parameters, frontal-plane TF alignment and ML compartment contact locations, have been defined. These parameters influence model-predicted ML compartment contact forces by altering how muscle forces and external loads pass relative to each compartment. Furthermore, frontal-plane TF alignment affects the loading of the knee [24]. Figure 1.5 shows how these parameters have been defined: In both the graphic and schematic, the red axis is perpendicular to the frontal plane, the green axis is perpendicular to the transverse plane, and the blue axis is perpendicular to the sagittal plane. The “Delp Knee Joint”

defines the sagittal plane TF translations and rotations specified by [10] (blue cylinder in B). Two joints (red cylinders), acting in the frontal plane, connect the sagittal articulation frame (translucent) to both the ML compartments (purple). By acting in parallel, these two revolute joints share all loads transmitted between the femur and tibia and resolve the ML contact forces required to balance the net reaction forces and frontal-plane moments across the TF joint. The medial compartment is fixed to the tibial plateau with a weld joint, and the lateral compartment is fixed to the tibial plateau with a weld constraint (black locks). Correspondingly, the knee remained a single DOF joint with articulation only in the sagittal plane. The locations of the ML compartments can be specified on a subject-specific basis (d1 and d2 in the inset graphic and schematic). revolute Similarly, the model's TF alignment can be specified (θ1 and θ2 in the inset graphic and schematic) by modifying the weld joint between the femur and femoral component and the weld joint between the tibial plateau and tibia.

Key similarities between the models of DeMers and Lerner [16-17] are:

- Identical sagittal plane rotations and translations of tibia and patella relative to the femur.
- A ball-and-socket joint at each hip.
- A revolute ankle joint.

The changes incorporated in Lerner [17] include:

- Augmented mechanism defining TF kinematics.
- distal femoral component and a tibial plateau body. Between these two bodies have been defined as a series of joints to characterize the TF kinematics and ML load distribution.
- Medial and lateral compartments welded at the anteroposterior midpoint of the tibial plateaus such that they remained fixed to the tibia while articulating with the surface of the femoral component during flexion-extension.
- A sagittal articulation frame body articulating between the femoral and the ML tibiofemoral components.

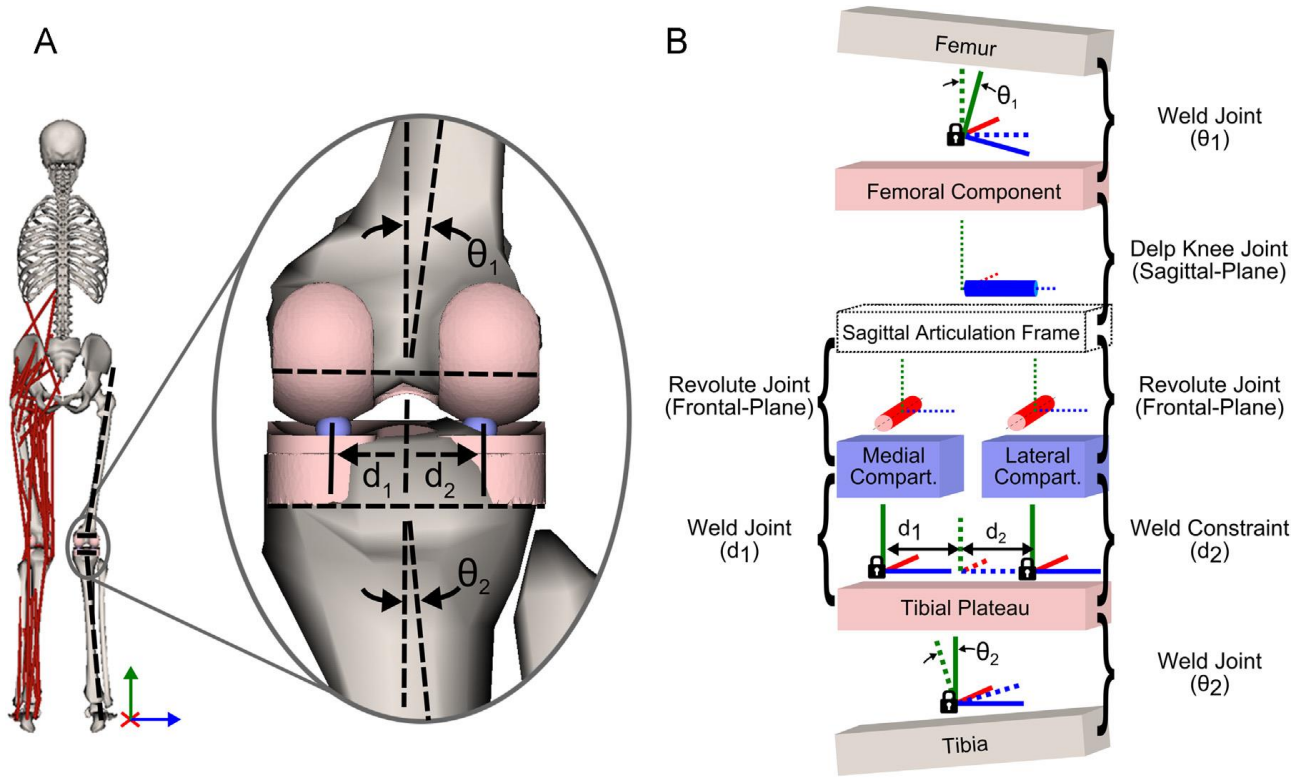

Figure 1.5: *Graphical (A) and schematic (B) depictions of the medial/lateral compartment joint structures in [17] musculoskeletal model.*

The specification of subject-specific model parameters in Lerner [17] model improves accuracy for what concerns gait analysis but the model is limited to a flexion angle range similar to gait and, thus, may not be appropriate for high knee flexion exercises such as cycling, elliptical, and rowing.

A recent model was developed for high flexion exercises, the Lai [18] model, its drawback is that it's not able to estimate medial and lateral tibial contact forces.
This model originates from Rajagopal [19], in which the musculotendinous unit (MTU) cylindrical wrapping surfaces have been introduced to improve the simulation speed.
These two models born because during many movements, such as the swing phase of running and the upstroke of pedaling the hips and knees are flexed more than 90° and these high flexion ranges brought the existing lower extremity models to have three important limitations. The most troubling limitation is that existing models greatly overestimated the passive fiber forces developed by the hip and knee extensors, most notably when the joints were flexed and the muscles were stretched.
These large passive forces could lead to anomalous compensatory muscle activity in muscle-driven simulations [19]. Another limitation was that the 3D paths of some muscles were poorly represented over the ranges of hip and knee angles commonly achieved by subjects during running, pedaling, and other movements. For example, in the Rajagopal model [19] the knee flexion moment arm of

the lateral gastrocnemius is diminished, and the moment arm of the biceps femoris short head surprisingly switches from flexion to extension, when the knee is flexed outside the model's recommended 120° operating range.

Yet another limitation is that the gastrocnemii and other muscles in these models become too short to generate active force during portions of the cycle that involve substantial hip and/or knee flexion. Thus, while many studies have used simulation-based approaches to gain valuable new insights into muscle function during walking [20], the limitations of existing models had to be resolved before such approaches could be reliably applied to a broader range of tasks.

The overarching aim of Lai model [18] was to develop a refined lower extremity model capable of producing plausible, muscle-driven simulations of fast running and pedaling, in addition to walking, from motion capture data and measured reaction forces.

It was observed that the anomalous co-activation of antagonist's muscles, commonly found in simulations of tasks involving high hip or knee flexion, was an unavoidable result of existing tracking algorithms [21]. Lai model [18] shows that the anomalous co-activation of antagonist's muscles can be reduced if the excessive passive forces generated by hip and knee extensors in the underlying model were diminished.

To reach out these results were made several important changes to the model published by Rajagopal [19], that involve the update of:

- TF kinematics;
- Relevant musculotendon paths;
- Tendon slack length for every muscle;
- Introduction of cylindrical wrapping surfaces for each MTU, these surfaces have been furtherly modified in respect to Rajagopal [19], so that the muscles' moment arms about the knee were more consistent with the moment arms published in literature with increasing knee flexion.;
- Optimal fiber length for 22 MTU (11 per leg).

Eventually, the Key differences between the models of Lerner and Lai [17-18], compared in this study, are:

- MusculoTendinous Unit (MTU) cylindrical wrapping surfaces,
- Increased the range of knee flexion.

- Updated paths of knee muscles and modified the force-generating properties of several muscles.

1.1 Study Goals

Computational motion analysis is a fundamental point in human motion studies, where optimizing accuracy and ease of use is a crucial point. For this reason, this study aims to prove the bounty of the ML load partitioning proposed by Lerner [17]. The hypothesis is that ML loads during cycling are equally shared among the two compartments, while gait shows a heavier medial engagement. [25, 26]

The possibility of using a single model to analyze exercises implying both normal and high knee flexion angles is a further interesting goal that this study proposes to investigate. To reach this goal tibiofemoral contacts load, net muscle moments and muscle forces predictions of both models have been analyzed and, since it hasn't been provided so far, this study aims to produce a comparison of the two proposed model. Since Lai model [18] is optimized for knee High Flexion (HF) angles it is considered as golden standard for the cycling trials comparison.

As merging condition has also been considered the complexity of the model, considering the effort to transfer complex computational items as bodies and muscles.

CHAPTER 2

MATERIALS AND METHODS

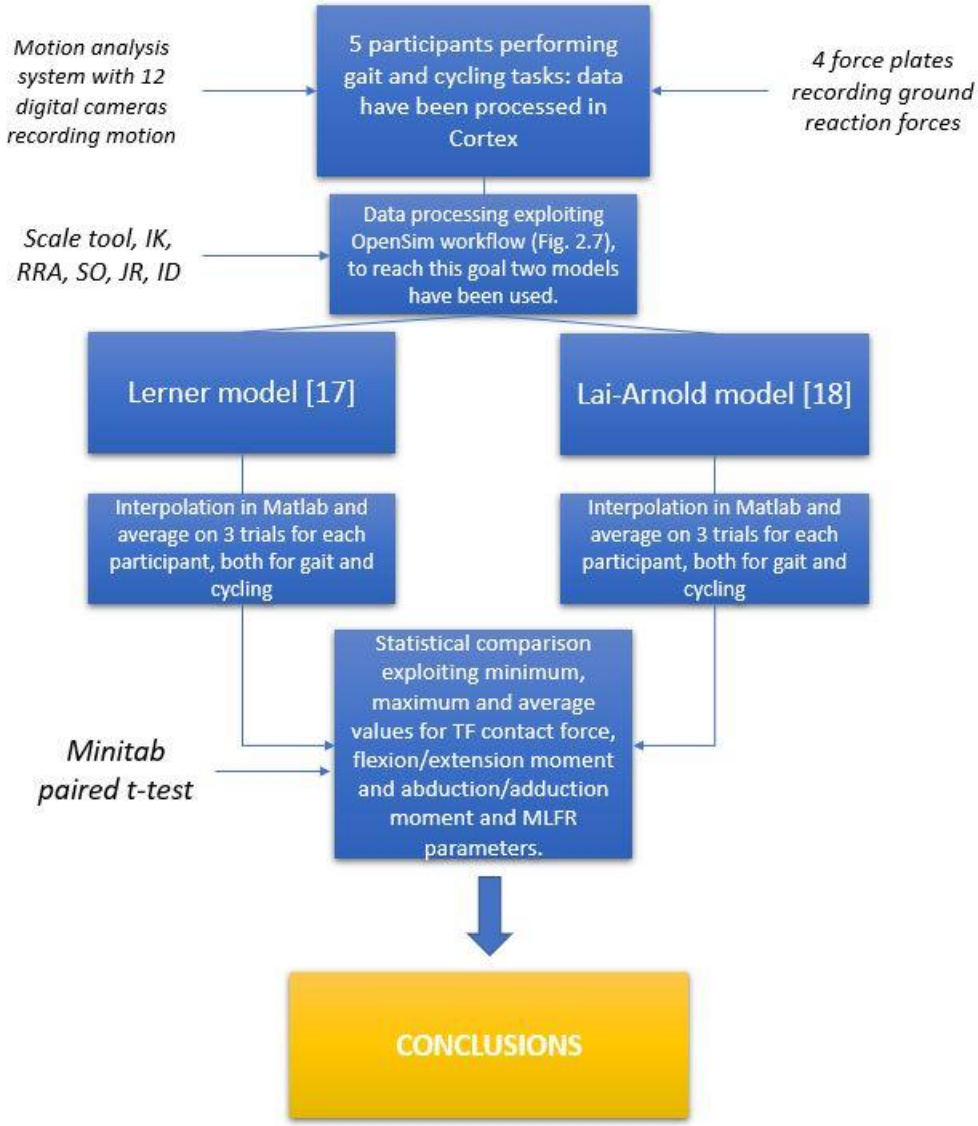

Figure 2.1. *Project workflow*

2.1 Participants and instrumentation

2.1.1 Participants

Data have been provided by HMB (Human Motion Biomechanics) Lab Review Board and were already processed in Cortex.

The experimental data have been used to perform a comparison among the two models, the study has been conducted with 5 participants. Before the test, each subject was required to sign and compile an Informed consent Form, the PAR-Q (Physical Activity Readiness Questionnaire) and an Information Form. In this last questionnaire, the subject declared the absence of physical activity earlier in the day of the experiment, the absence of pregnancy or of any attempt to become pregnant, was reported also if he/she had any medication, any respiratory or chronic diseases. The information summarized in Table 1 has been reported in the information form document as well.

Subject ID	Age [years]	Gender	Height [cm]	Weight [lb]	Mass [kg]	Dominant leg
2018Mar01-01	23	M	183	212,3	96,3	Left
2018Jan19-01	22	M	181,6	174,28	79,05	Right
2018Apr24-01	23	M	162,6	123,9	56,2	Right
2018Apr27-01	21	M	164,5	142,75	64,75	Right
2018Jun08-01	21	F	171,5	151,46	68,7	Right

Table 2.1: *Data summary with the information about the participants of the study.*

The first column contains the subject IDs that represent essentially the day of the experiment and the number of the subject in the day. The format is the following: YYYYMonDD−## (e.g. the experiment of the first subject in the Table below was the March 01, 2018 and the subject was the first that day).

In the second column of the Table, it is reported the age of each subject in years. The HMB Lab protocol says that subjects must be between 18 and 40 years of age and the inclusion criterion is therefore respected. In particular, the age is between 21 and 23 with a mean age of 22 (± 0,894) years. In the third column is reported the gender of the subjects. Only one subject was female and four were males. The higher number of male subjects is irrelevant for the study being conducted because the difference between males and females isn't investigated and it isn't a goal of the research. The fourth and the fifth columns show, respectively, the height in centimeters and the weight in pounds as they have been measured. Then conversion to kilograms is done (1 lb = 0,453592 Kg) and the results are reported in the sixth column.

In the last column, the dominant leg of each subject is reported. This is an important characteristic because the results were obtained only in the dominant leg side. It's an important feature because influences the pattern of the acquisition, for example if the subject has a right dominant leg, his/her recorded walking is left, right, left foot, the opposite holds true for a left dominant leg.

To understand which the dominant leg was, has been asked the participant which would have been the leg used to kick a ball [39].

2.1.2 Equipment

Data were collected using a motion analysis system (Motion Analysis Corp. Santa Rosa, CA, USA) consisting of the following: (1) twelve (6 Owl, 3 Osprey, 2 Kestrel, 1 Eagle) digital cameras (Motion Analysis); (2) Cortex software (Version 7.01, Motion Analysis) for calibration, setup, data collection, and post-processing; (3) 20 mm retroreflective markers (Motion Analysis); (4) 4 ground forces plates (Accugait, AMTI, Watertown, MA, USA) that measured time-dependent ground reaction forces and moments aligned in a walkway; (5) a stationary bike (Lifecycle GX, Life Fitness, Schiller Park, IL, USA) retrofitted with custom pedals containing 6-axis load cells (AMTI, Watertown, MA, USA) with markers attached to track pedal orientation and relate local load cell coordinate system to the Cortex coordinate system; The cameras tracked marker trajectories within the capture volume and kinematic data were recorded in Cortex software at a frequency of 150 Hz. The kinetic data from the force plates for gait, and load cells for cycling, were captured at a frequency of 150 Hz and synchronized with kinematic data within Cortex.

As already told, for cycling experiments was used a stationary bike. This bike could be adjusted according to the size of the subject. Both pedals were instrumented with load cells, markers and a strap were added. This was useful to have full contact between the foot and the load cells for the entire experiment. It was important to strap the subjects tightly enough for them not to be able to slip, but not too tight such that it was uncomfortable for the subject.

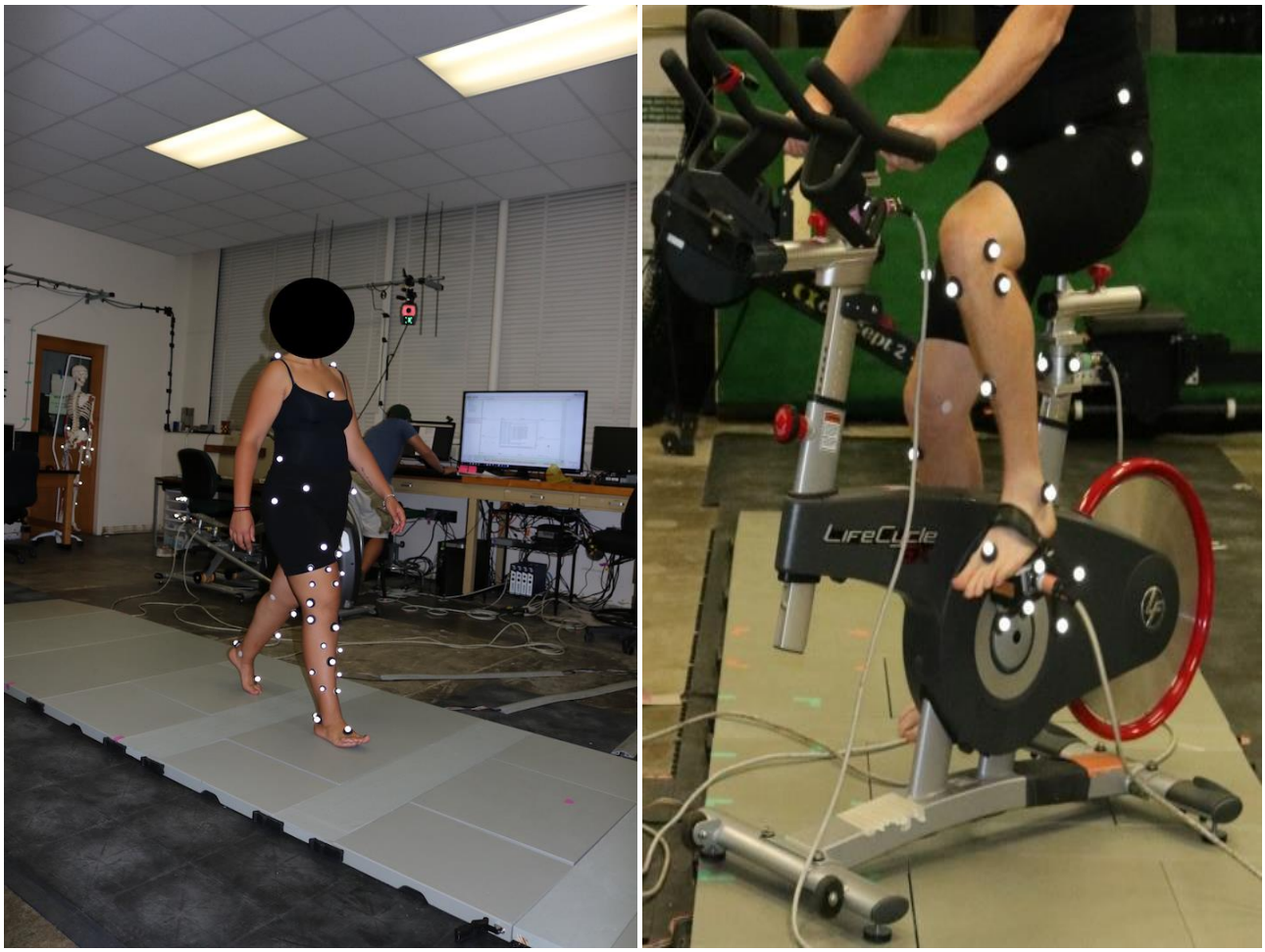

Figure 2.2: *Equipment setup for gait (left) and cycling (right) experiments.*

For the experiments, passive markers were used. The markers had plastic support and they were covered by reflective material. The infrared light, from the cameras, hit the markers. They reflected this light and the cameras could only see the markers and not the entire segment where they were placed. They had a spherical shape and this allowed to improve infrared rays reflection. They were used in two different sizes (12 mm and 20 mm). The smaller ones were placed in the region of the knee when the subject was particularly small and there was no place for the others.
Velcro tape was used to adhere the markers to the skin. In particular, on the skin of the subject were placed stickers that on one side had Velcro. This was used to attack the marker.

In the experiments force plates (and load cells) were used to obtain the reaction forces between the foot and the ground or between the foot and the pedals of the bike.
Gait experiments were conducted using three ground force plates (Accugait, AMTI, Watertown, MA, USA). The force plates were placed in a staggered way in the lab (see the left part of Figure 2.3). They had three sensors in each corner with four different local systems.

Using the data from each corner, the six components of the total reaction forces and moments were calculated (Fx, Fy, Fz, Mx, My and Mz). NetForce software, combined with AMTI multi-axis force platforms, helped the users to visualize and save data from the transducers [27]. In Figure 2.3 reported below, the digital system and the analog system components are represented. In the digital system, each force plate was connected to the AMTI PJB-101 with a RJ cable. The AMTI PJB-101 was a box that had the only purpose of creating an interface between the sensors and the computer. In the middle of the same Figure 2.3, there is the PJB-101 box; it needed to be powered and connected to the RS-232 computer connection with a RS-232 serial cable. This cable was needed to transmit information to and from the main computer where
NetForce software for analyzing and visualizing the data was installed [28]. The analog system was used to connect and exploit the data of the force plates in Cortex software. In the upper part of Figure 2.3, the analog connections are reported.

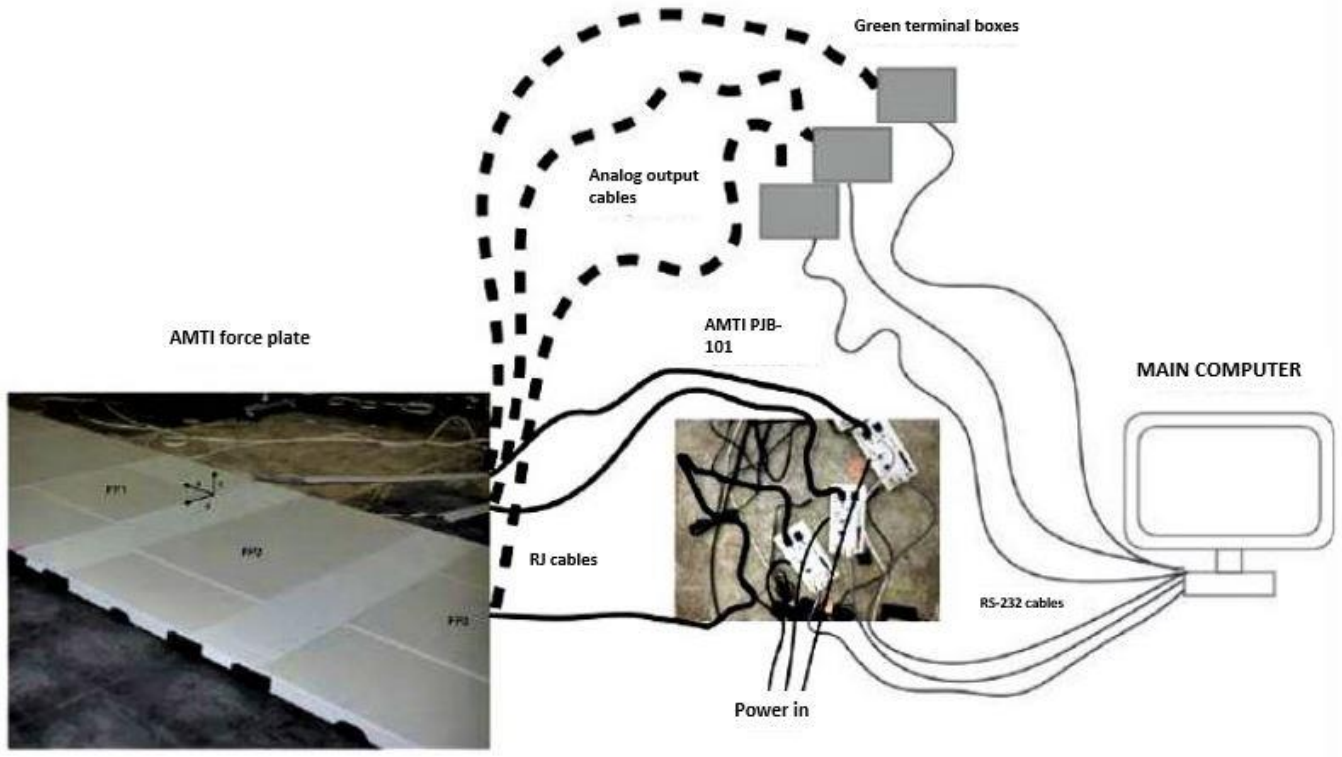

Figure 2.3: *Force Plates analog and digital systems with the AMTI PJB- 101 and the main computer.*

The load cells were transducers that measured forces in x, y and z directions and the moments around these axes [29, 30]. In total, there were six outputs. The sensors were strain gages. When a force was applied to a structure, the structure modified slightly its dimensions resulting in the detection of a strain. Strain gauges were based on the property to change resistance when they were

strained. They were placed in a Wheatstone bridge configuration, in this way applying a voltage at the input was possible to get an output voltage dependent on the applied force.
Because this force strained the structure, the resistance changed and with it the output voltage. There was the need to amplify the signal, then the load cells were connected to the GEN5 signal conditioner through a 26 pins circular type connector. The GEN5 signal conditioner conditioned the signal from six strain gages and was able to provide six conditioned output signals, either digital or analog (in this case digital) [31]. The signal conditioning included amplification, filtering and periodic sampling of the data [31]. The information was sent to the main computer, via the digital system, through an USB connector.

2.2 Softwares for data post-processing

2.2.1 MATLAB

MATLAB (MathWorks, Natick, MA, USA) is a matrix-based language for programming and, nowadays, it is one of the most used among researchers and engineers, also because of the ease of access and interpretability of its desktop environment [32]. It this research, MATLAB codes have been written and used with the following purposes:

- To exploit the linear interpolation function, interpolating the gait and cycling trials on 1001 time points.
- To average the results over three full cycles for each participant, both for gait and cycling.

In gait analysis the cycle is normalized time from first heel strike (0%) to next heel strike (100%). The zero value of the knee flexion range is intended as the fully extended knee.
For cycling analysis '[%] Cycle' is normalized time from the first top dead center (0%) to second top dead center (100%). The zero value of the knee flexion range is intended as the fully extended knee here as well.

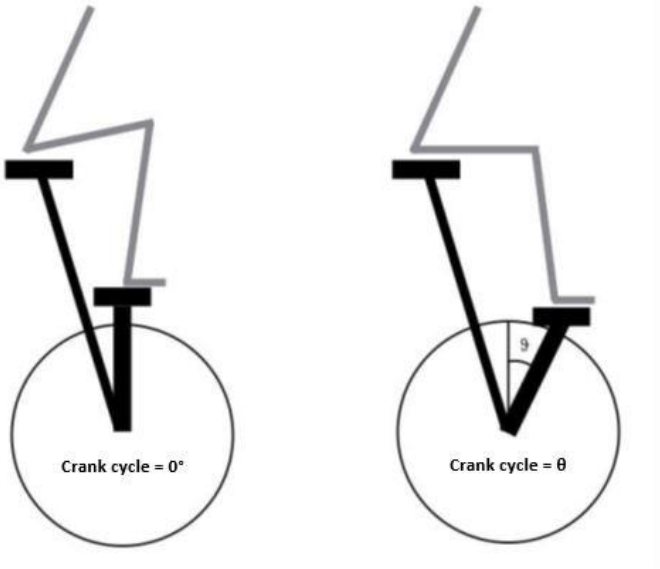

Figure 2.4. *Definition of cycling cycle with crank angle.*

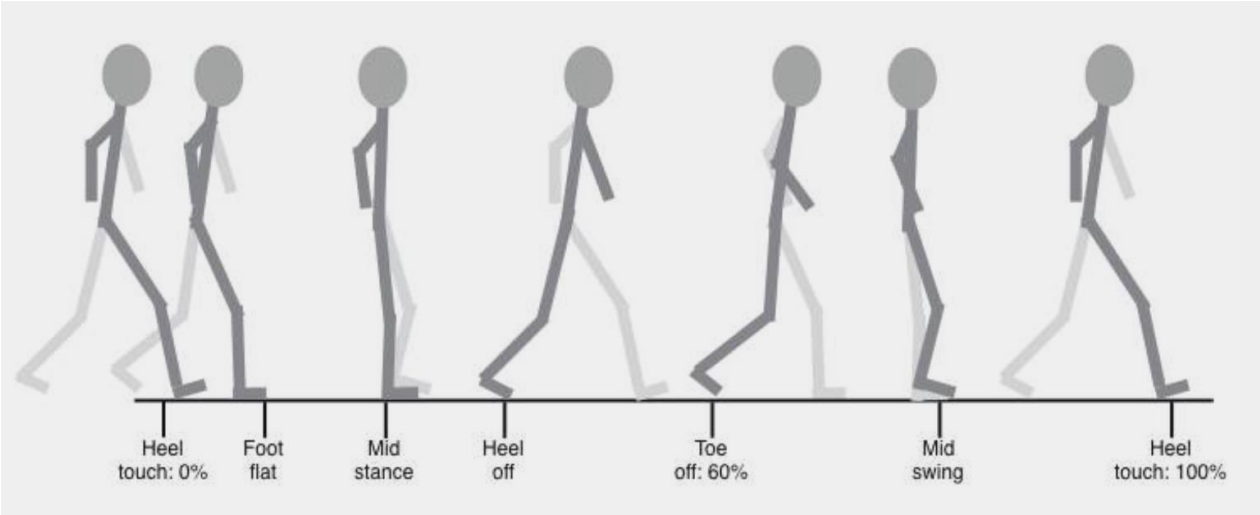

Figure 2.5. *Definition of gait cycle.*

2.2.2 OpenSim

OpenSim (OpenSim, Palo Alto, CA, USA) is open-source software for dynamic simulations with neuromuscular models of the human body. The software is written in ANSI C++. A graphical user interface (GUI) was written (see Figure 2.6 reported below where the OpenSim user interface, with a model loaded, is reported), in Java language, to facilitate interaction with the user [10, 33]. This allows the user that isn't skilled in computer science to use the program without any particular difficulty. An open-source tool for visualization, that consists of a class library written in C++, is integrated into with the software: the Visualization Toolkit (VTK) from Kitware [10, 33, 34].

OpenSim includes different tools that have been used in this research. They will be described in detail in the next section. Here, only an initial introduction to the software is given. OpenSim allows scaling the model depending on our subject's weight and height.

OpenSim's scale tool, Inverse Kinematics (IK) and Inverse Dynamics (ID) solver, Static Optimization (SO) tool and finally Joint Reaction (JR) analysis have been used to model the recorded activity.

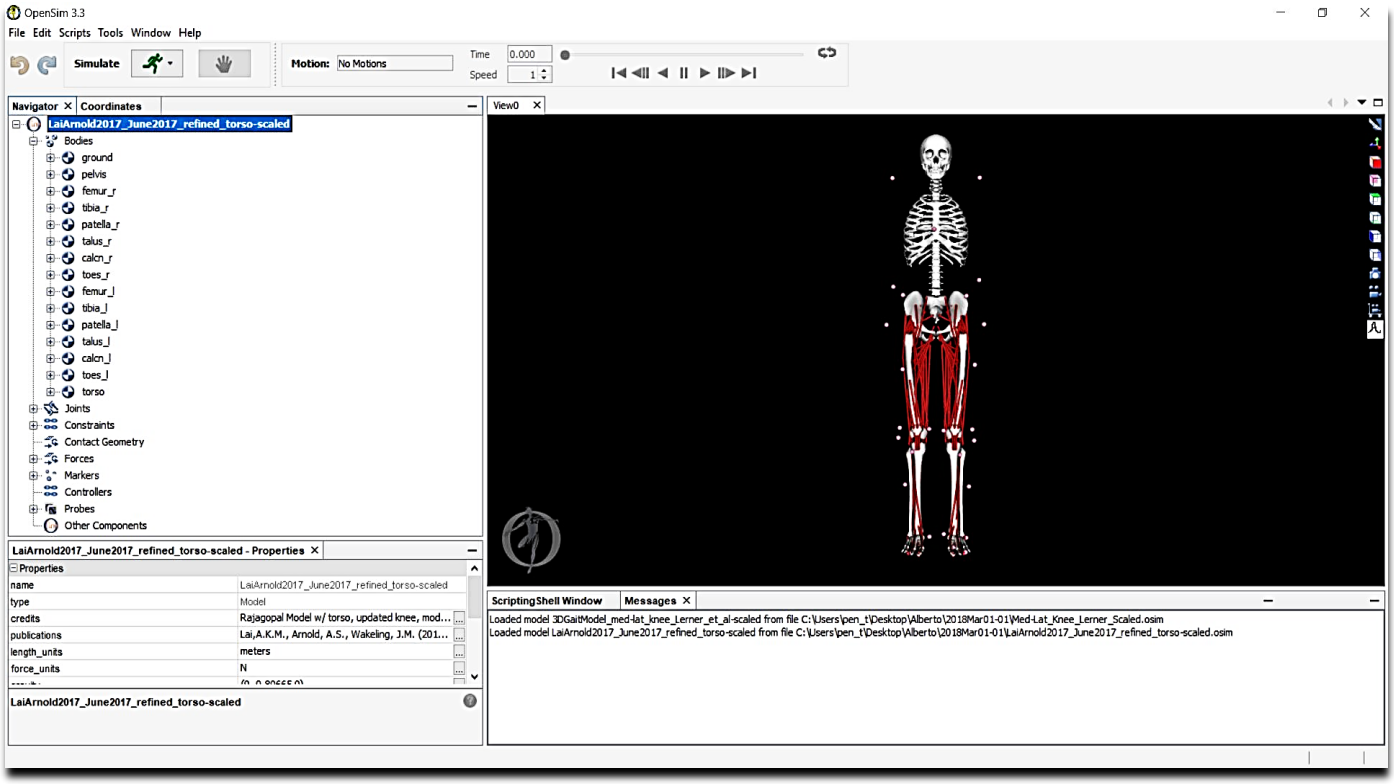

Figure 2.6: *OpenSim Graphical user interface with a model loaded.*

2.3 OpenSim analysis

OpenSim is an open-source musculoskeletal modeling environment developed by Stanford University to allow researchers to determine forces and moments internal to the body. This tool is invaluable compared to traditional inverse dynamics calculations because it considers the loads at the body's joints due to muscle activation. Without accounting for such loads, proper determination of joint contact forces would be impossible. Model selection is one of the most important choices in the OpenSim environment and this research attempted to define which are the most important differences in gait and cycling among Lai [17] and Lerner [18], to reach this goal each participant was processed through the OpenSim workflow. The OpenSim workflow contains five crucial steps which are shown in Figure 2.7 and will be outlined in more detail below.

The parameters compared through paired t-test in the statistical analysis are obtained from inverse dynamics, among which are present flexion/extension moment and abduction/adduction moment, as well as from joint reaction analysis, from which TF contact forces have been predicted. These parameters have been evaluated in their maximum, minimum and average values.
Another important parameter is the ML tibiofemoral Force Ratio (MLFR) defined as:

$$MLFR = \frac{Medial\ TF\ contact\ force}{Lateral\ TF\ contact\ force} \qquad (2.1)$$

It has been considered only for Lerner [17] since the ML tibiofemoral contact loads partition is a particular feature of this model. This parameter has been compared considering only its maximum value.
Fundamentally, the most important comparison criterion is the one considering maximum values because the average value prediction should be similar for both the models since they both originate from the study of DeMers [16] and the minimum values difference should be of negligible order of magnitude.
Figure 2.8 shows an example of a cycling participant in OpenSim. The Helen Hayes marker set used to define the position of the skeleton in OpenSim is the same used Cortex. The markers are displayed as white dots in the picture and pink dots in OpenSim. The red lines in the OpenSim image show approximations of human muscles. OpenSim will use the activation of these muscles to drive the model's motion in later processing.

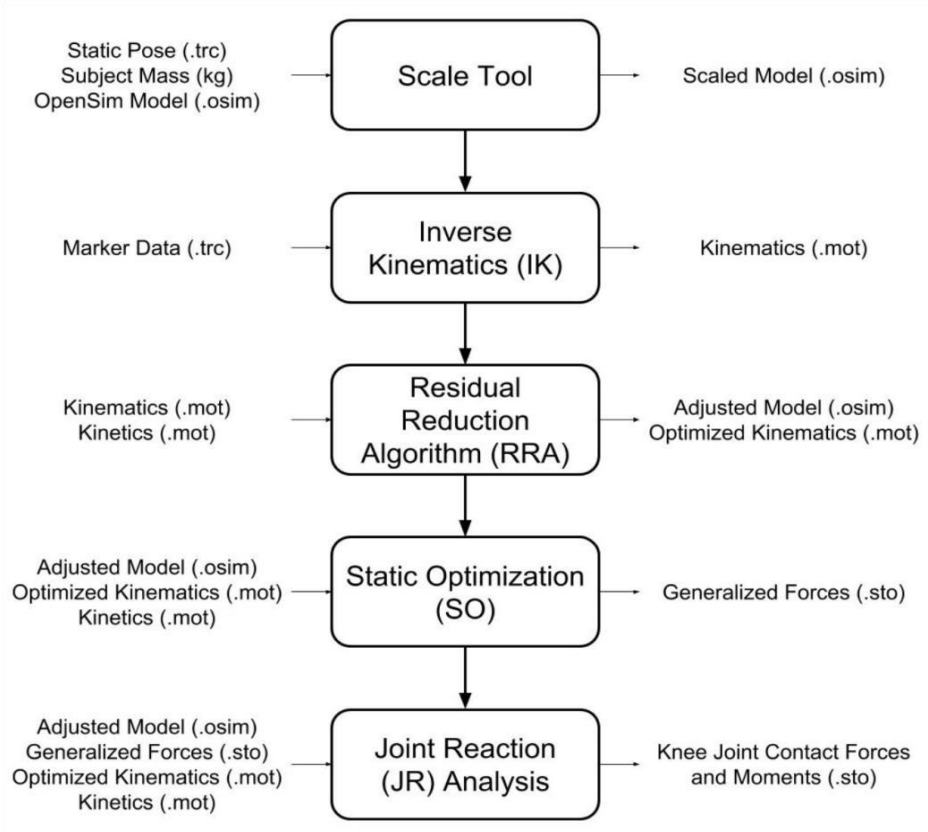

Figure 2.7: *Flowchart of the five analysis tools used in OpenSim processing. The inputs to each tool are shown on the left with outputs shown on the right.*

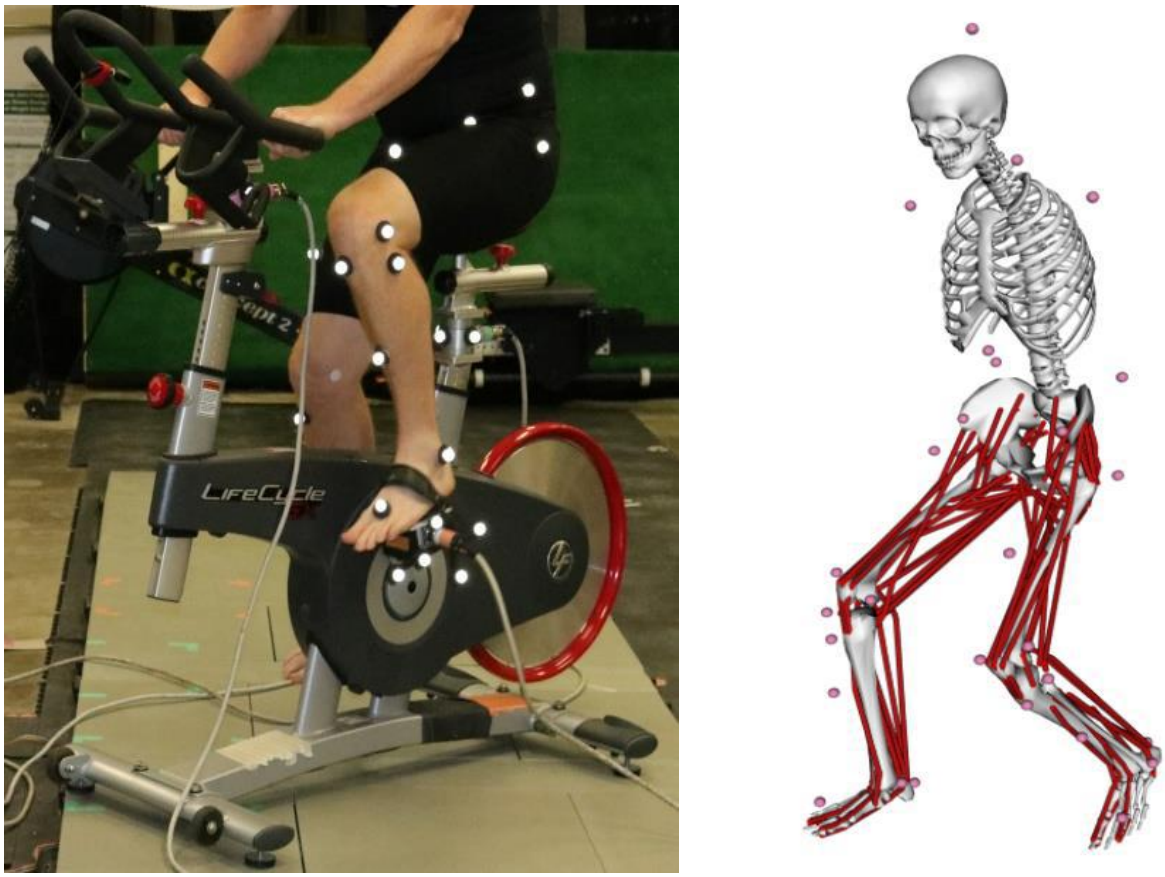

Figure 2.8: *Cycling participant showed mid-trial (left) and processed in OpenSim (right).*

2.3.1 Scale tool

The scale tool allows for the creation of a subject-specific model. Each OpenSim model has a generic height and weight assigned to it as well as generic body segment lengths and mass distributions. To get accurate simulation results, the generic model must be "scaled" to better match the real participant. This is achieved by first moving virtual markers on the generic model to locations better representing the positions of the actual markers placed on the participant. When the scale tool is run, OpenSim manipulates the generic model to match the virtual markers as closely as possible to the experimental markers provided from the static trial. This is typically an iterative process that requires the virtual markers in the generic model to be manually moved many times. Iteration continues until the largest absolute error between each virtual and experimental marker pair is under 0.02 m. If this criterion is met and the resulting model does not exhibit any non-physiological joint rotations, the model is considered scaled.

2.3.2 Inverse Kinematics

IK is the first tool that is applied to a subject specific scaled model. The purpose of the IK tool is to translate the dynamic cycling trial data into the OpenSim environment. This is accomplished by analyzing each frame of the '.trc' file and placing the scaled model in an orientation that best aligns the virtual and experimental markers. A weighted squared error method is used to find the optimum balance between all of the markers. This process is similar to the Scale Tool except in IK, the model's dimensions are fixed. Once the entire trial is processed, the IK tool outputs a results file that contains the model's optimal joint trajectories.

2.3.3 Residual Reduction Algorithm

The RRA tool is responsible for attempting to merge the kinematics from IK with the load data from the ground reaction forces (GRFs) measured experimentally. Discrepancies between the kinematics and the load cell data, due to both modeling and experimental errors, lead to the formation of large residual forces that OpenSim applies to the pelvic origin (Eq. 2.2).

$$F_{External} + F_{Residual} = \sum_{i=1}^{segments} m_i a_i \qquad (2.2)$$

These forces can at times be necessary, such as when they stand in for forces not accounted for experimentally but are considered by OpenSim to be errors. This is because OpenSim is primarily designed for analyzing gait in which no external loading beyond the GRFs is applied to the body. RRA, therefore, seeks to reduce the pelvic residuals by shifting the location of the torso mass center, rearranging the body segment mass distribution, and altering the IK results to better match what would be induced by the GRFs. The torso mass center is typically chosen as the body segment to adjust because it is the most massive and least easily estimated of the model. RRA has many outputs, but the one of most concern to this study is the reduced pelvic residuals optimized kinematics file which is fundamental to perform static optimization.

2.3.4 Static optimization

The SO tool breaks the motion of the body down into the result of individual muscle activations. The Lai model [18] contains 84 actuators while Lerner model [17] 92, that are responsible for simulating the behavior of the actual muscles in the human body. SO uses inverse dynamics to calculate the net joint moments for each frame in time. These moments are then broken down into resultant torques caused by the actuators. An algorithm that minimizes the sum of the squared muscle activations is used to determine the individual muscle forces. It is this step-in which model selection has the most important effect. The precise location of the actuators in the model along with their force properties has a large effect on the results from SO. After SO has analyzed the entire trial, it outputs a file containing all the activation forces of each muscle activator over time.

2.3.5 Joint reaction

JR is an OpenSim Analysis for calculating resultant forces and moments at the joint using the adjusted model and kinematics from RRA and the muscle activation forces from SO. The results from JR are the typical goal for most OpenSim experiments. Specifically, it calculates the joint forces and moments transferred between consecutive bodies as a result of all loads acting on the model. These forces and moments correspond to the internal loads carried by the joint structure. These loads represent the contributions of all un-modeled joint structures that would produce the desired joint kinematics, such as cartilage contact and any omitted ligaments. In this study, joint contact loads on each participant’s dominant knee were analyzed.

2.3.6 Inverse Dynamics

ID tool was used outside the OpenSim workflow, to obtain the net joint moments.

The Inverse Dynamics (ID) Tool determines the generalized forces (e.g., net forces and torques) at each joint responsible for a given movement. Given the kinematics (e.g., states of motion) describing the movement of a model and perhaps a portion of the kinetics (e.g., external loads) applied to the model, the ID Tool uses these data to perform an inverse dynamic analysis. Classical mechanics mathematically expresses the mass-dependent relationship between force and acceleration, **F** = m**a**, with equations of motion. The Inverse Dynamics Tool solves these equations, in the inverse dynamics sense, to yield the net forces and torques at each joint which produce the movement.

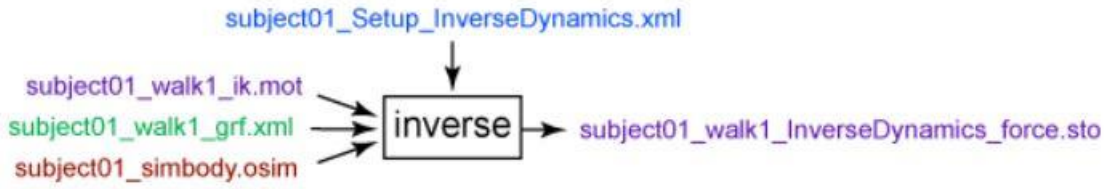

Figure 2.9: Required inputs and outputs for the Inverse Dynamics Tool.

It uses the kinematic data from IK and the external load data (i.e. ground reaction forces, moments, and center of pressure location) measured experimentally. The Inverse Dynamics Tool generates a single file in a folder specified in the setup file: **subject01_walk1_InverseDynamics_force.sto**, which is a storage file containing the time histories of the net joint torques and forces acting along the coordinate axes that produce the accelerations estimated (via double differentiation) from your measured experimental motion and the external forces applied.

The '**subject01_Setup_InverseDynamics.xml**' is a setup file that offers the possibility to save the setting preferences among which can be provided the paths of the input files showed in figure 2.9.

2.4 Statistical analysis

The statistical analysis is performed in Minitab. The paired t-Student test is conducted to determine if a statistical difference between the samples is present. The statistical significance is set with $p<0,05$.

CHAPTER 3

RESULTS

In this chapter the plots of the results with related statistical analysis are reported. Reported graphs are about total TF contact force, flexion/extension moment, abduction/adduction moment each reported both for cycling and gait trials. The first paragraph also report MLFR statistics, the last shows forces produced by the muscles more involved in the production of TF loads during cycling.

3.1 Lerner model ML contact forces

The model used to perform this analysis, defined in Lerner [17], was 'uninformed', this means that the generic frontal-plane locations of the medial/lateral compartment structures were 20 mm medial and lateral of the knee joint center. The tibiofemoral alignment for this model at 180°.
For the following graphs forces are in Newton, normalized by each participant's body weight.
In gait analysis '[%] Cycle' is normalized time from first heel strike (0%) to next heel strike (100%). The zero value of the knee flexion range is intended as the fully extended knee.
For cycling analysis '[%] Cycle' is normalized time from the first top dead center (0%) to second top dead center (100%). The zero value of the knee flexion range is intended as the fully extended knee here as well.
Results reported are 2018Mar01-01, 2018Jan19-01, 2018Apr24-01, 2018Apr27-01 and 2018Jun08-01 participants averaged.

Paired T-Test and CI: Gait (Max); Cycling (Max)

Descriptive Statistics

Sample	N	Mean	StDev	SE Mean
Gait (Max)	5	4,30	2,66	1,19
Cycling (Max)	5	0,93	0,21	0,09

Estimation for Paired Difference

Mean	StDev	SE Mean	95% CI for μ_difference
3,37	2,64	1,18	(0,10; 6,65)

μ_difference: mean of (Gait (Max) - Cycling (Max))

Test

Null hypothesis	H_0: μ_difference = 0
Alternative hypothesis	H_1: μ_difference ≠ 0

T-Value	P-Value
2,86	0,046

Figure 3.1. *Maximum MLFR paired T-test comparison.*

Maximum MLFR ($p < 0,05$) paired t-test comparison gave significantly different results for gait compared to cycling, with gait showing maximum medial contact force 4 times higher than cycling. Cycling presents a more equal distribution of the force, with an average of the maximum MLFR of 0,93.

Furthermore, looking at the knee flexion angle graphs can be stated that gait trials never cross 70° flexion, for this reason, the angles crossing this value have been defined as ‘High Flexion (HF) angles’.

3.1.1 Gait

The figure below shows the graph describing the TF contact force during a full gait cycle on the right, while on the left is reported the knee flexion angle. Two force peaks can be noticed, according to what reported in [40] they are in correspondence of the contralateral toe-off and contralateral heel-strike.

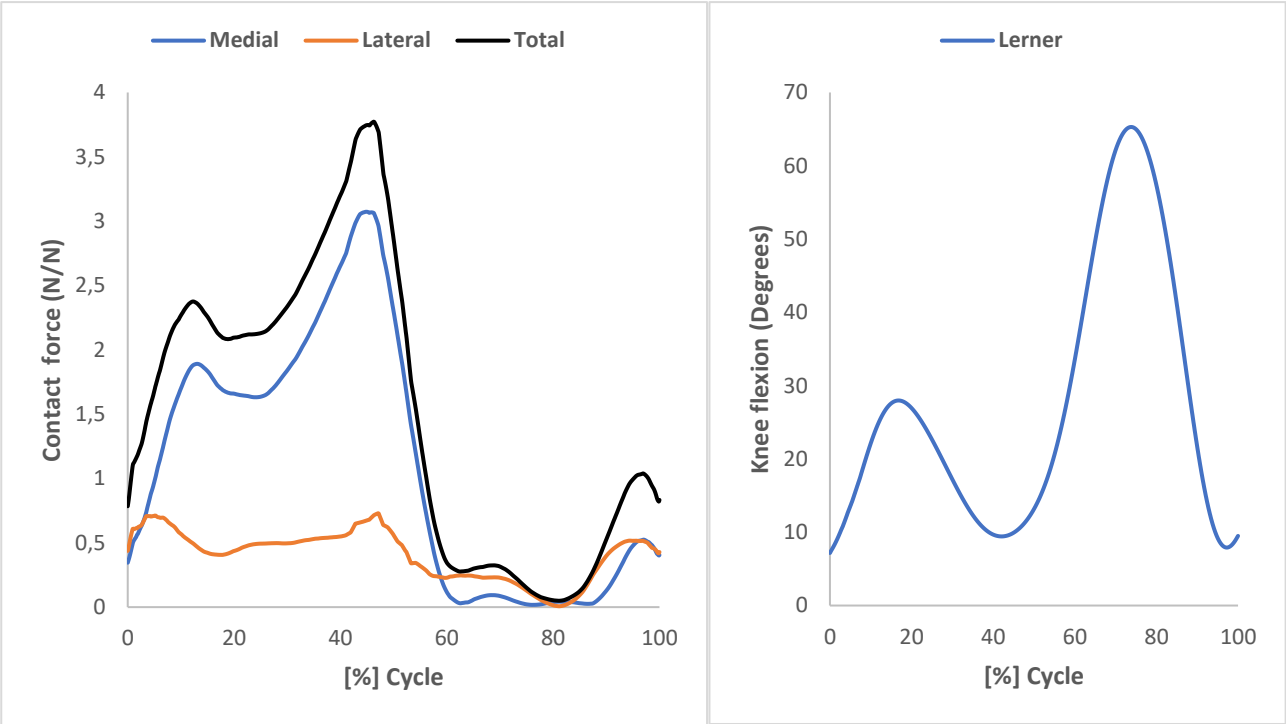

Figure 3.2. *Tibial contact forces (left) and averaged knee flexion angle (right) during gait, computed with Lerner [17] model.*

3.1.2 Cycling

The figure below shows the TF contact force during a full cycling cycle on the left, with the related knee flexion angle on the right.

According to what reported in [41] The first peak occurrs during the pedal downstroke around 80° of knee flexion the second and smaller peak occurrs at maximal extension, prior to the upward movement of the leg.

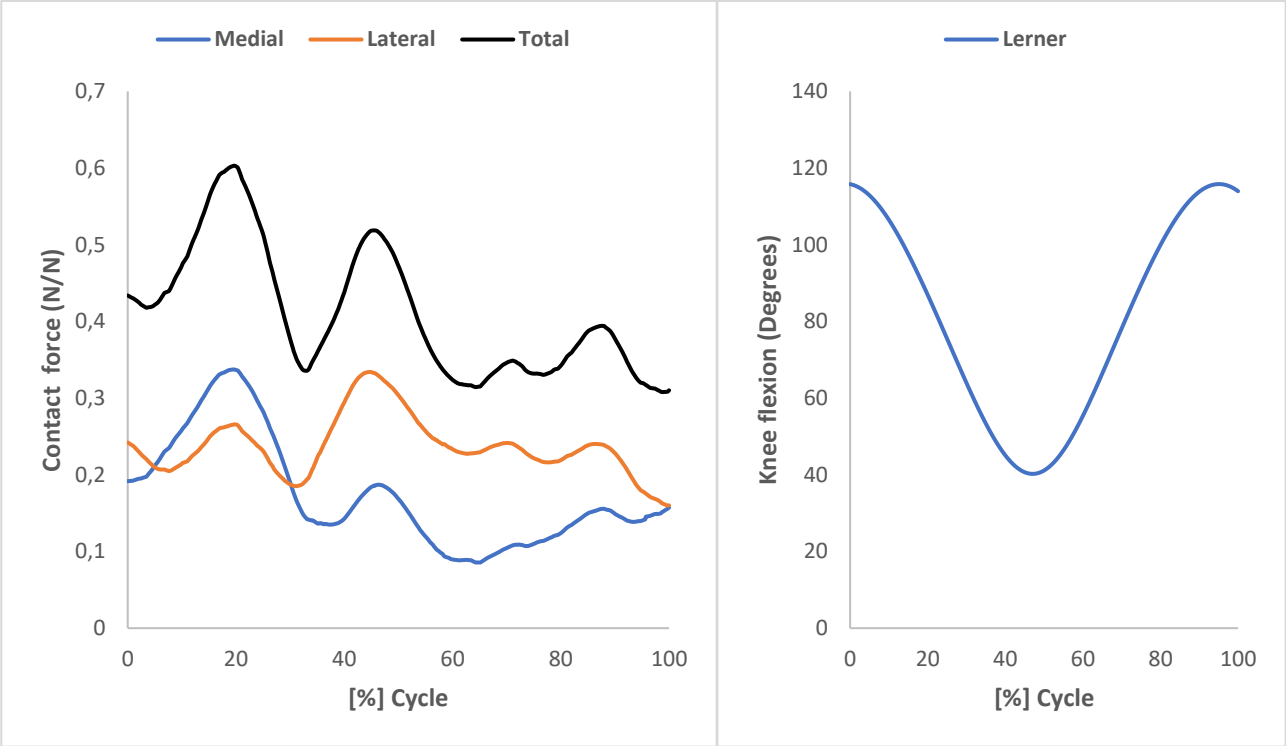

Figure 3.3: *Tibial contact forces (left) and averaged knee flexion angles (right) during cycling, computed with Lerner [17] model.*

3.2 Lerner and Lai-Arnold models total TF contact forces

For the following graphs forces are in Newton, normalized by each participant's body weight.
In gait analysis '[%] Cycle' is normalized time from first heel strike (0%) to next heel strike (100%). The zero value of the knee flexion range is intended as the fully extended knee.
For cycling analysis '[%] Cycle' is normalized time from the first top dead center (0%) to second top dead center (100%). The zero value of the knee flexion range is intended as the fully extended knee here as well.
The following graphs shows each participant contribution to both cycling and gait tasks after having them averaged on three trials for each participant.

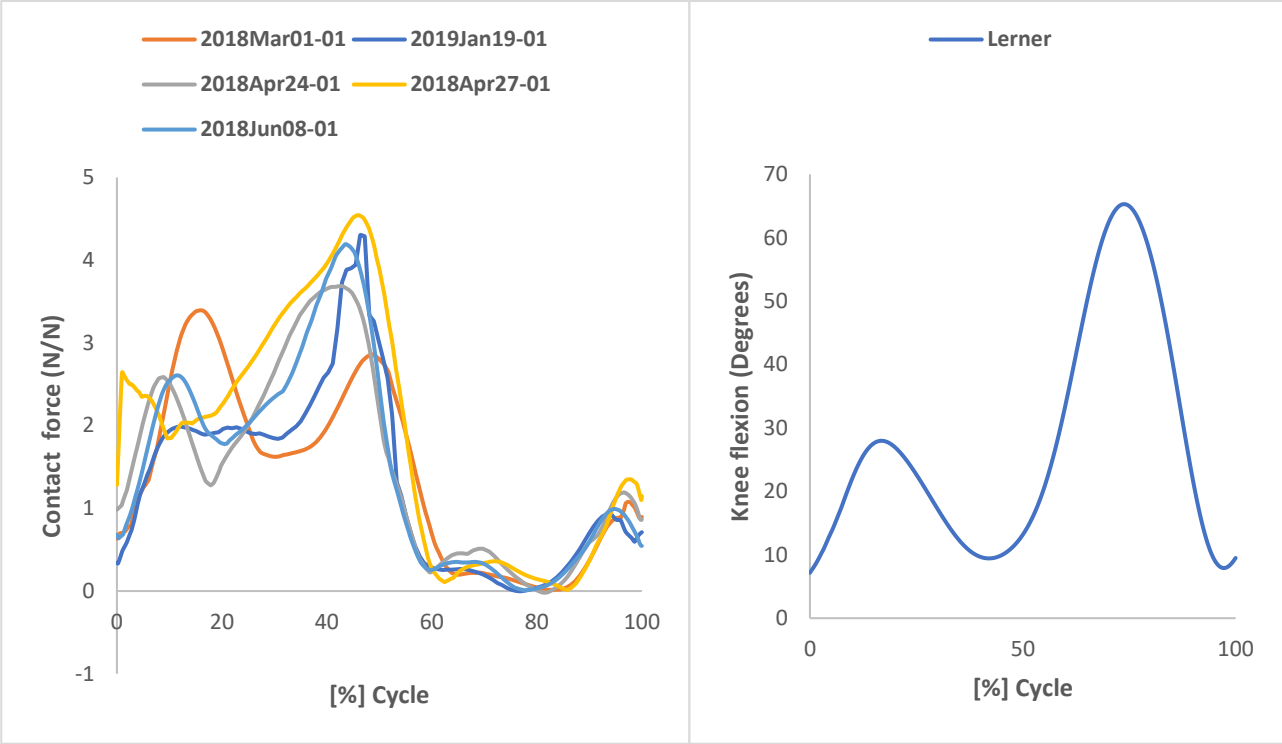

Figure 3.4: *Total tibial contact forces (left) and averaged knee flexion angle (right) during gait, computed with Lerner model [17].*

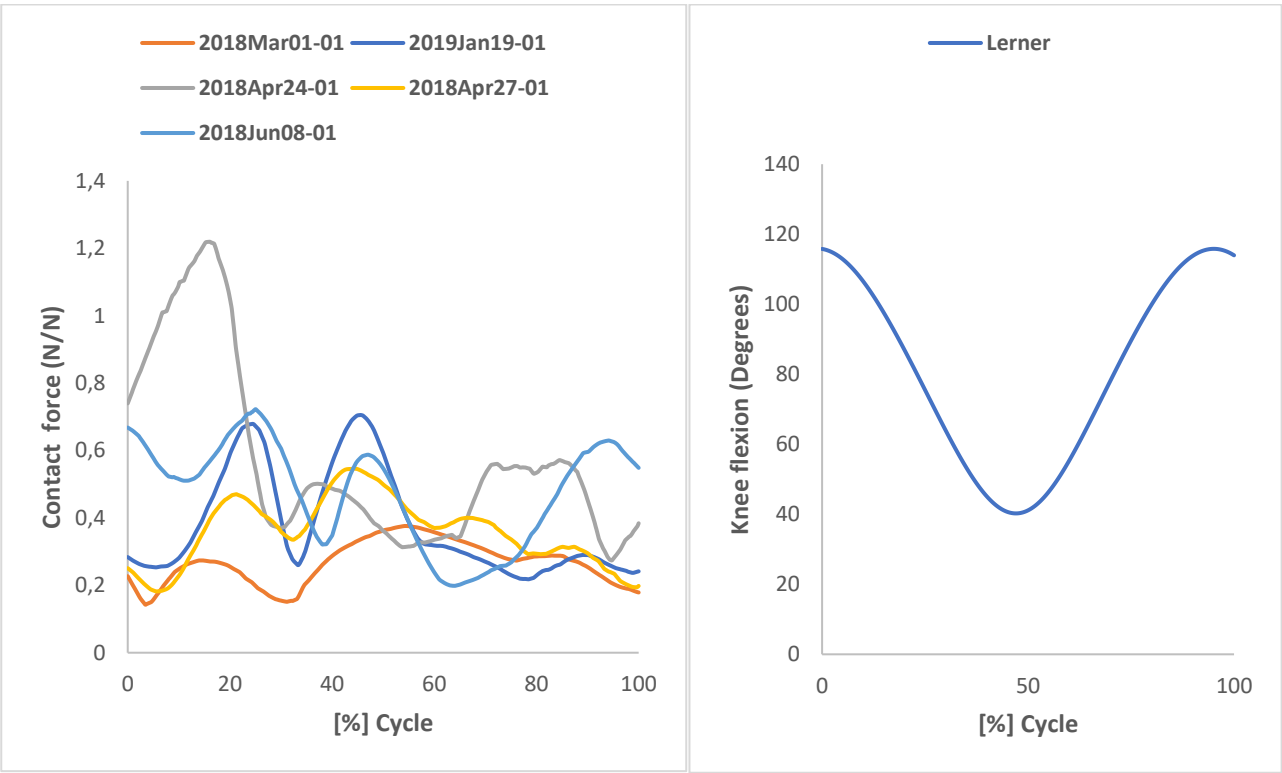

Figure 3.5: *Total tibial contact forces (left) and averaged knee flexion angles (right) during cycling, computed with Lerner model [17].*

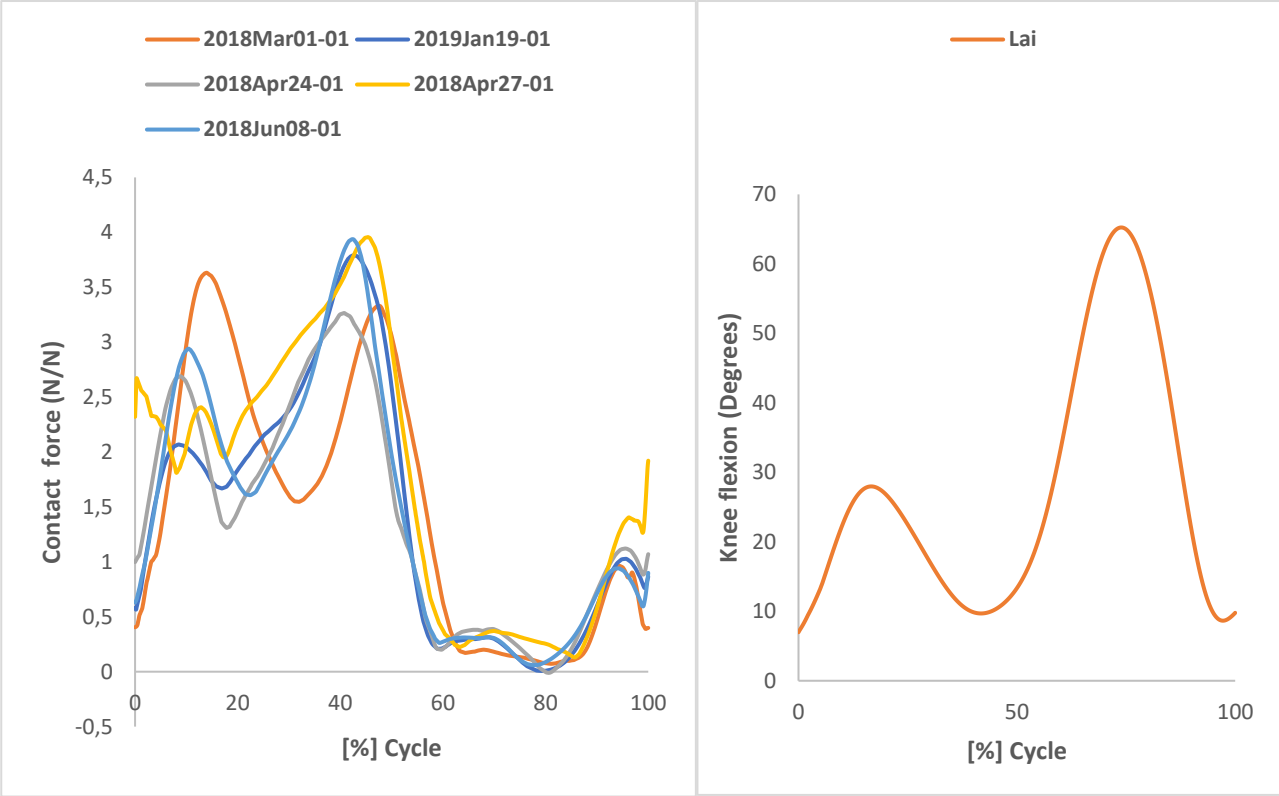

Figure 3.6: *Total tibial contact forces (left) and averaged knee flexion angles (right) during gait, computed with Lai model [18].*

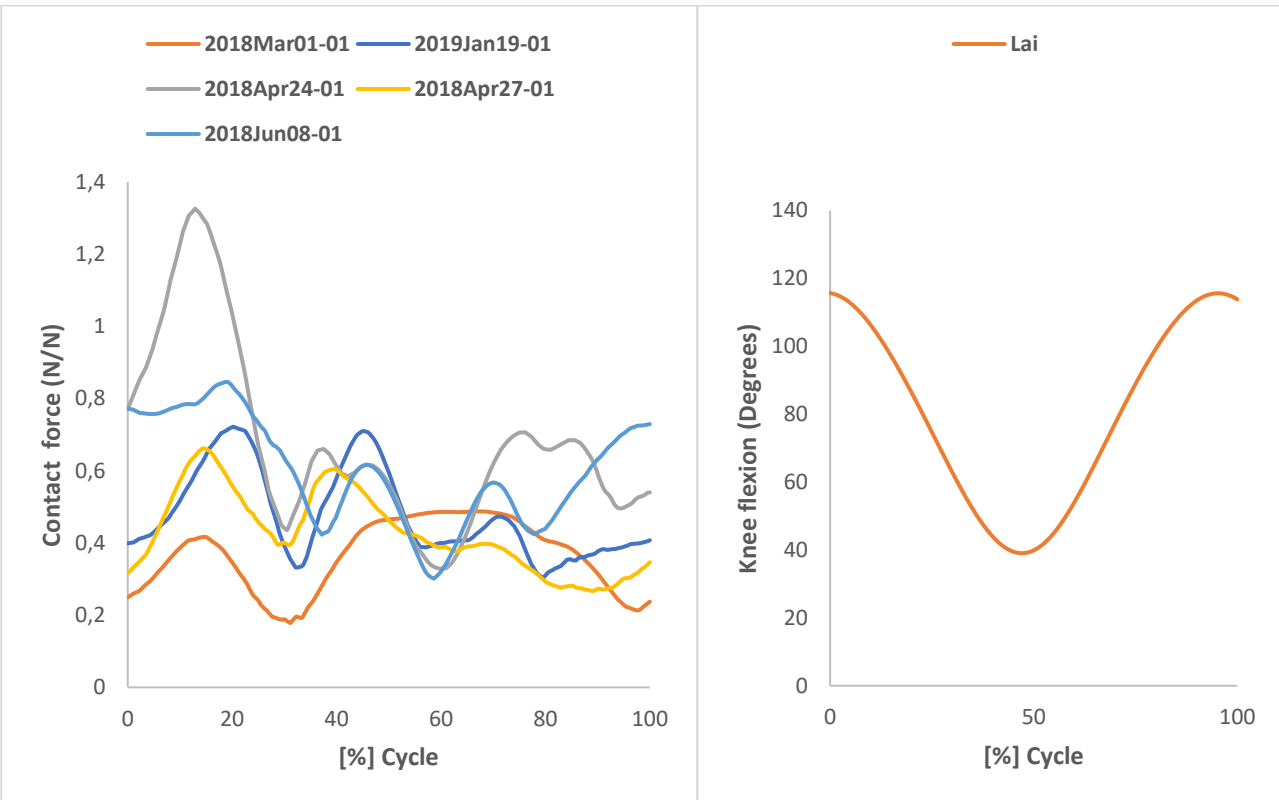

Figure 3.7: *Total tibial contact forces (left) and averaged knee flexion angles (right) during cycling, computed with Lai model [18].*

3.2.1 Averaged gait TF contact forces

The maximum, minimum and average TF contact force ($p > 0,05$) during gait wasn't significantly different for Lerner [17] compared to Lai [18].

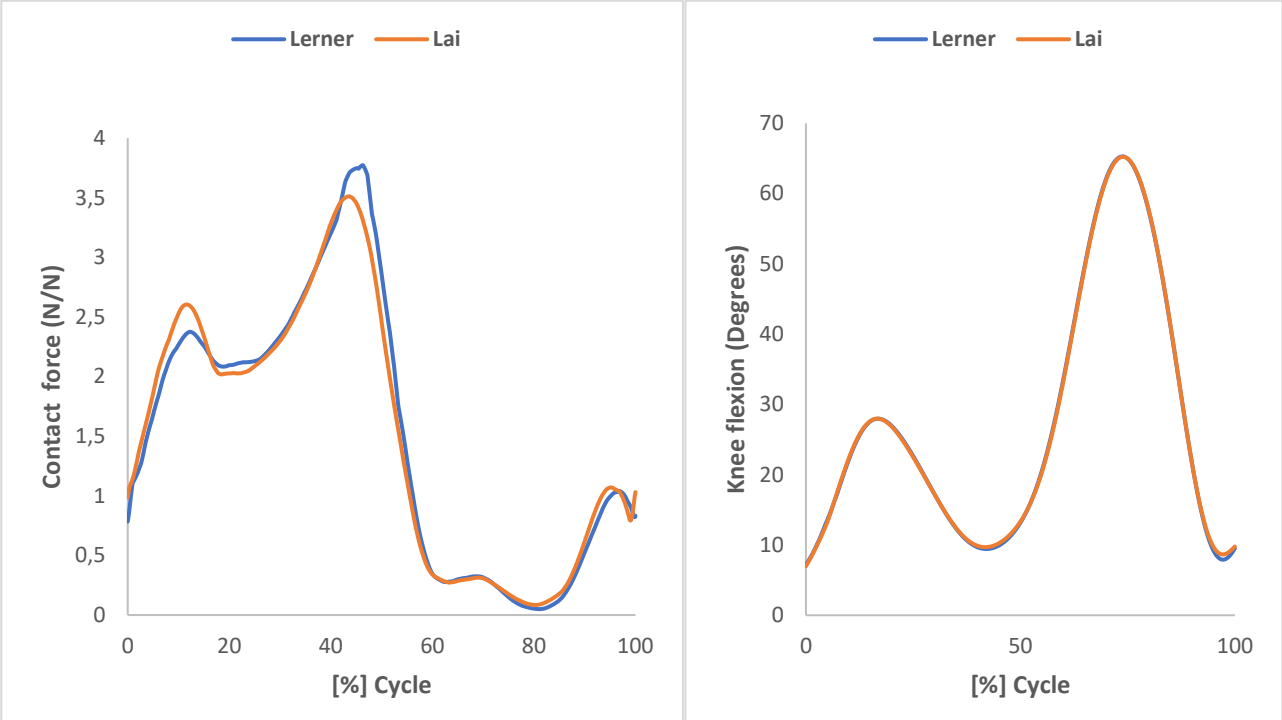

Figure 3.8: *Total tibial contact forces (left) and knee flexion angles (right) during gait, computed averaging the 5 participant results both with Lerner [17] and Lai [18] models.*

Paired T-Test and CI: Ler (Avg); Lai (Avg)

Descriptive Statistics

Sample	N	Mean	StDev	SE Mean
Ler (Avg)	5	1,5208	0,1992	0,0891
Lai (Avg)	5	1,5085	0,1339	0,0599

Estimation for Paired Difference

Mean	StDev	SE Mean	95% CI for μ_difference
0,0122	0,1017	0,0455	(-0,1140; 0,1385)

μ_difference: mean of (Ler (Avg) - Lai (Avg))

Test

Null hypothesis H_0: μ_difference = 0
Alternative hypothesis H_1: μ_difference ≠ 0

T-Value	P-Value
0,27	0,801

Paired T-Test and CI: Ler (Max); Lai (Max)

Descriptive Statistics

Sample	N	Mean	StDev	SE Mean
Ler (Max)	5	4,024	0,471	0,211
Lai (Max)	5	3,716	0,284	0,127

Estimation for Paired Difference

Mean	StDev	SE Mean	95% CI for μ_difference
0,308	0,329	0,147	(-0,101; 0,717)

μ_difference: mean of (Ler (Max) - Lai (Max))

Test

Null hypothesis H_0: μ_difference = 0
Alternative hypothesis H_1: μ_difference ≠ 0

T-Value	P-Value
2,09	0,104

Figure 3.9. *Average (left) and maximal (right) total tibial contact force paired t-test comparison.*

Paired T-Test and CI: Ler (Min); Lai (Min)

Descriptive Statistics

Sample	N	Mean	StDev	SE Mean
Ler (Min)	5	0,0031	0,0147	0,0066
Lai (Min)	5	0,0515	0,0559	0,0250

Estimation for Paired Difference

Mean	StDev	SE Mean	95% CI for μ_difference
-0,0484	0,0435	0,0194	(-0,1023; 0,0056)

μ_difference: mean of (Ler (Min) - Lai (Min))

Test

Null hypothesis	H_0: μ_difference = 0
Alternative hypothesis	H_1: μ_difference ≠ 0

T-Value	P-Value
-2,49	0,068

Figure 3.10. *Minimal total tibial contact force paired t-test comparison.*

3.2.2 Averaged cycling TF contact forces

The maximum, minimum and average TF contact force ($p < 0,01$) during cycling was significantly different for Lerner [17] compared to Lai [18].

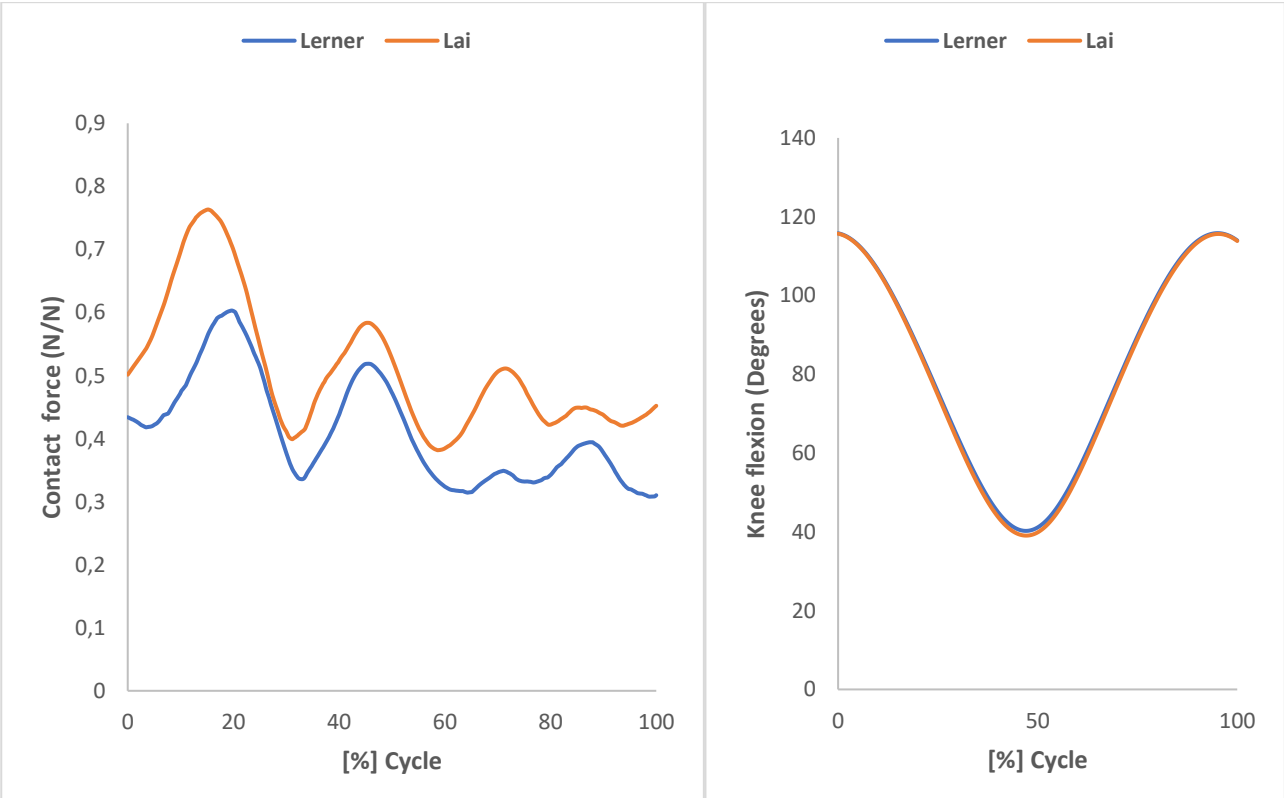

Figure 3.11: *Total tibial contact forces (left) and knee flexion angles (right) during cycling, computed averaging the 5 participant results both with Lerner [17] and Lai [18] models.*

Paired T-Test and CI: Ler (Avg); Lai (Avg)

Descriptive Statistics

Sample	N	Mean	StDev	SE Mean
Ler (Avg)	5	0,4109	0,1169	0,0523
Lai (Avg)	5	0,5100	0,1277	0,0571

Estimation for Paired Difference

Mean	StDev	SE Mean	95% CI for μ_difference
-0,09916	0,01925	0,00861	(-0,12306; -0,07525)

μ_difference: mean of (Ler (Avg) - Lai (Avg))

Test

Null hypothesis H_0: μ_difference = 0
Alternative hypothesis H_1: μ_difference ≠ 0

T-Value	P-Value
-11,52	0,000

Paired T-Test and CI: Ler (Max); Lai (Max)

Descriptive Statistics

Sample	N	Mean	StDev	SE Mean
Ler (Max)	5	0,714	0,315	0,141
Lai (Max)	5	0,809	0,317	0,142

Estimation for Paired Difference

Mean	StDev	SE Mean	95% CI for μ_difference
-0,0947	0,0442	0,0198	(-0,1497; -0,0398)

μ_difference: mean of (Ler (Max) - Lai (Max))

Test

Null hypothesis H_0: μ_difference = 0
Alternative hypothesis H_1: μ_difference ≠ 0

T-Value	P-Value
-4,79	0,009

***Figure 3.12**. Average (left) and maximal (right) total tibial contact force paired t-test comparison.*

Paired T-Test and CI: Ler (Min); Lai (Min)

Descriptive Statistics

Sample	N	Mean	StDev	SE Mean
Ler (Min)	5	0,203	0,048	0,022
Lai (Min)	5	0,809	0,317	0,142

Estimation for Paired Difference

Mean	StDev	SE Mean	95% CI for μ_difference
-0,606	0,272	0,121	(-0,943; -0,269)

μ_difference: mean of (Ler (Min) - Lai (Min))

Test

Null hypothesis H_0: μ_difference = 0
Alternative hypothesis H_1: μ_difference ≠ 0

T-Value	P-Value
-4,99	0,008

***Figure 3.13.** Minimal total tibial contact force paired t-test comparison.*

3.3 Lerner and Lai-Arnold models total moments

For the following graphs, the considerations for the previous graphs are still valid. What changes here is that for the TF moments the forces used to define them are in Newton, normalized by each participant height multiplied by mass.

3.3.1 Gait

The maximum, minimum and average flexion/extension moment ($p > 0,1$) during gait wasn't significantly different for Lerner [17] compared to Lai [18], the same can be stated for adduction/abduction moment ($p > 0,1$).

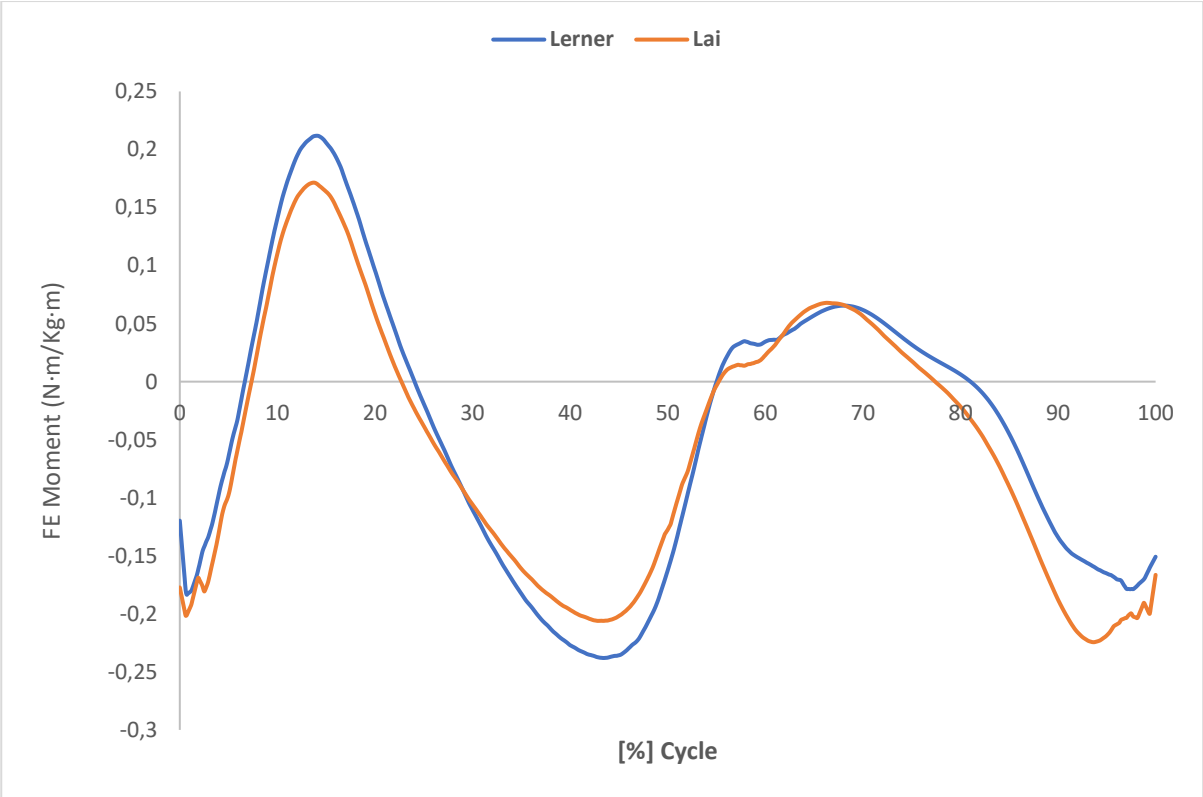

Figure 3.14: *Average flexion(-)-extension(+) knee joint net muscle moment during gait, computed with Lerner [17] and Lai [18] models.*

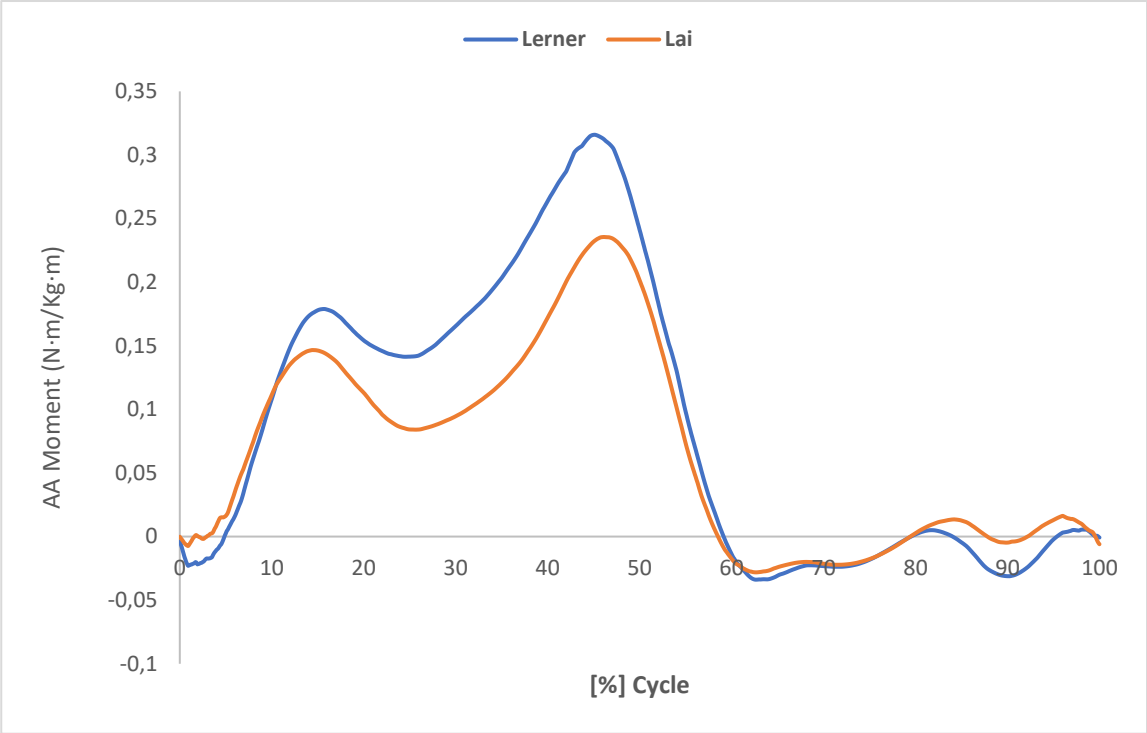

Figure 3.15: *Average abduction(+)-adduction(-) knee joint net muscle moment during gait computed with Lerner [17] and Lai [18] models.*

Paired T-Test and CI: Ler (Avg); Lai (Avg)

Descriptive Statistics

Sample	N	Mean	StDev	SE Mean
Ler (Avg)	5	-0,0444	0,0955	0,0427
Lai (Avg)	5	-0,0576	0,0503	0,0225

Estimation for Paired Difference

Mean	StDev	SE Mean	95% CI for μ_difference
0,0132	0,0607	0,0272	(-0,0622; 0,0886)

μ_difference: mean of (Ler (Avg) - Lai (Avg))

Test

Null hypothesis	H_0: μ_difference = 0
Alternative hypothesis	H_1: μ_difference ≠ 0

T-Value	P-Value
0,49	0,652

Paired T-Test and CI: Ler (Avg); Lai (Avg)

Descriptive Statistics

Sample	N	Mean	StDev	SE Mean
Ler (Avg)	5	0,0869	0,0309	0,0138
Lai (Avg)	5	0,0655	0,0323	0,0145

Estimation for Paired Difference

Mean	StDev	SE Mean	95% CI for μ_difference
0,0214	0,0292	0,0131	(-0,0149; 0,0577)

μ_difference: mean of (Ler (Avg) - Lai (Avg))

Test

Null hypothesis	H_0: μ_difference = 0
Alternative hypothesis	H_1: μ_difference ≠ 0

T-Value	P-Value
1,64	0,176

Figure 3.16*. Average knee flexion/extension (left) and abduction/adduction moments (right) paired t-test comparison.*

Paired T-Test and CI: Ler (Max); Lai (Max)

Descriptive Statistics

Sample	N	Mean	StDev	SE Mean
Ler (Max)	5	0,2457	0,2041	0,0913
Lai (Max)	5	0,1857	0,1358	0,0608

Estimation for Paired Difference

Mean	StDev	SE Mean	95% CI for μ_difference
0,0601	0,1526	0,0682	(-0,1294; 0,2496)

μ_difference: mean of (Ler (Max) - Lai (Max))

Test

Null hypothesis H_0: μ_difference = 0
Alternative hypothesis H_1: μ_difference ≠ 0

T-Value	P-Value
0,88	0,428

Paired T-Test and CI: Ler (Max); Lai (Max)

Descriptive Statistics

Sample	N	Mean	StDev	SE Mean
Ler (Max)	5	0,3243	0,0808	0,0362
Lai (Max)	5	0,2401	0,0761	0,0340

Estimation for Paired Difference

Mean	StDev	SE Mean	95% CI for μ_difference
0,0843	0,1034	0,0462	(-0,0441; 0,2126)

μ_difference: mean of (Ler (Max) - Lai (Max))

Test

Null hypothesis H_0: μ_difference = 0
Alternative hypothesis H_1: μ_difference ≠ 0

T-Value	P-Value
1,82	0,142

Figure 3.17. *Maximal knee flexion/extension (left) and abduction/adduction (right) moments paired t-test comparison.*

Paired T-Test and CI: Ler (Min); Lai (Min)

Descriptive Statistics

Sample	N	Mean	StDev	SE Mean
Ler (Min)	5	-0,2975	0,1085	0,0485
Lai (Min)	5	-0,2862	0,0757	0,0338

Estimation for Paired Difference

Mean	StDev	SE Mean	95% CI for μ_difference
-0,0113	0,1002	0,0448	(-0,1357; 0,1131)

μ_difference: mean of (Ler (Min) - Lai (Min))

Test

Null hypothesis H_0: μ_difference = 0
Alternative hypothesis H_1: μ_difference ≠ 0

T-Value	P-Value
-0,25	0,813

Paired T-Test and CI: Ler (Min); Lai (Min)

Descriptive Statistics

Sample	N	Mean	StDev	SE Mean
Ler (Min)	5	-0,04862	0,01607	0,00718
Lai (Min)	5	-0,04286	0,02016	0,00902

Estimation for Paired Difference

Mean	StDev	SE Mean	95% CI for μ_difference
-0,00576	0,00952	0,00426	(-0,01758; 0,00606)

μ_difference: mean of (Ler (Min) - Lai (Min))

Test

Null hypothesis H_0: μ_difference = 0
Alternative hypothesis H_1: μ_difference ≠ 0

T-Value	P-Value
-1,35	0,247

Figure 3.18. *Minimal knee flexion/extension (left) and abduction/adduction (right) moments paired t-test comparison.*

3.3.2 Cycling

The maximum, minimum and average flexion/extension moment ($p > 0,1$) during cycling wasn't significantly different for [17] compared to [18], the same can be stated for adduction/abduction moment ($p > 0,1$).

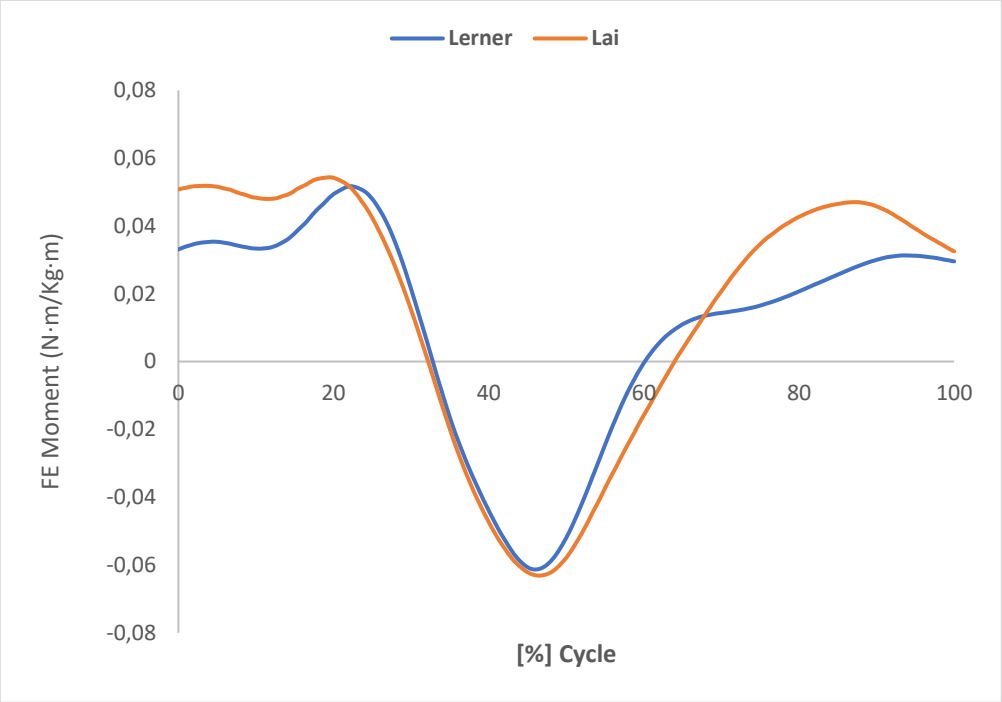

Figure 3.19: *Average flexion(-)-extension(+) knee joint net muscle moment during Cycling, computed with Lerner [17] and Lai [18] models.*

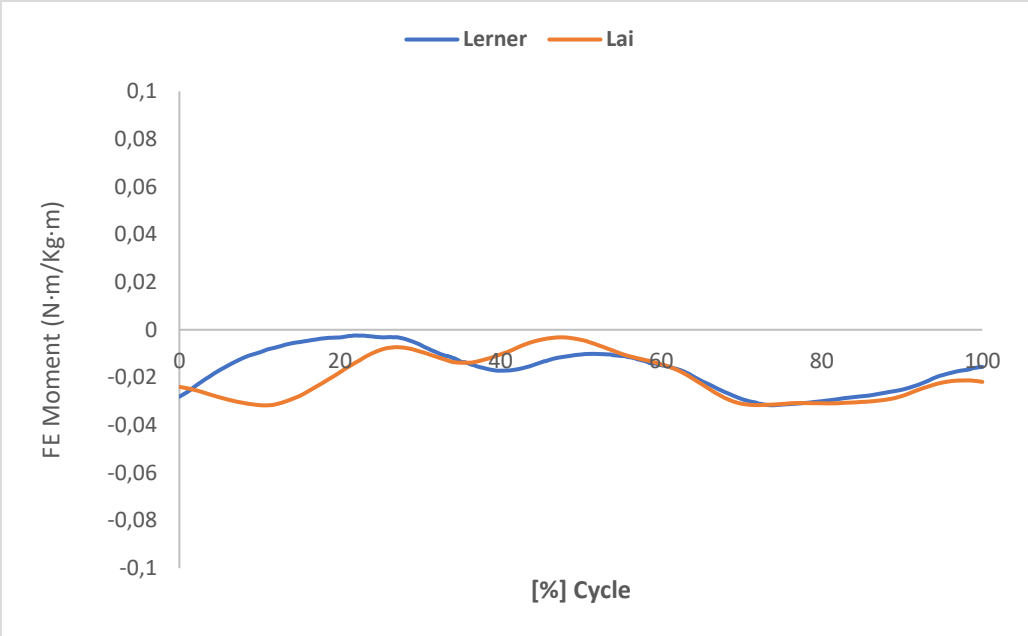

***Figure 3.20**: Average abduction(+)-adduction(-) knee joint net muscle moment during Cycling computed with Lerner [17] and Lai [18] models.*

Paired T-Test and CI: Ler (Avg); Lai (Avg)

Descriptive Statistics

Sample	N	Mean	StDev	SE Mean
Ler (Avg)	5	0,01045	0,00927	0,00414
Lai (Avg)	5	0,01489	0,01954	0,00874

Estimation for Paired Difference

Mean	StDev	SE Mean	95% CI for μ_difference
-0,00444	0,01286	0,00575	(-0,02041; 0,01153)

μ_difference: mean of (Ler (Avg) - Lai (Avg))

Test

Null hypothesis	H_0: μ_difference = 0
Alternative hypothesis	H_1: μ_difference ≠ 0

T-Value	P-Value
-0,77	0,483

Paired T-Test and CI: Ler (Avg); Lai (Avg)

Descriptive Statistics

Sample	N	Mean	StDev	SE Mean
Ler (Avg)	5	-0,01644	0,01528	0,00683
Lai (Avg)	5	-0,01994	0,01305	0,00584

Estimation for Paired Difference

Mean	StDev	SE Mean	95% CI for μ_difference
0,00350	0,00398	0,00178	(-0,00145; 0,00844)

μ_difference: mean of (Ler (Avg) - Lai (Avg))

Test

Null hypothesis	H_0: μ_difference = 0
Alternative hypothesis	H_1: μ_difference ≠ 0

T-Value	P-Value
1,96	0,121

***Figure 3.21.** Average knee flexion/extension (left) and abduction/adduction moments (right) paired t-test comparison..*

Paired T-Test and CI: Ler (Max); Lai (Max)

Descriptive Statistics

Sample	N	Mean	StDev	SE Mean
Ler (Max)	5	0,0605	0,0259	0,0116
Lai (Max)	5	0,0771	0,0488	0,0218

Estimation for Paired Difference

Mean	StDev	SE Mean	95% CI for μ_difference
-0,0166	0,0415	0,0185	(-0,0681; 0,0349)

μ_difference: mean of (Ler (Max) - Lai (Max))

Test

Null hypothesis	H_0: μ_difference = 0
Alternative hypothesis	H_1: μ_difference ≠ 0

T-Value	P-Value
-0,90	0,421

Paired T-Test and CI: Ler (Max); Lai (Max)

Descriptive Statistics

Sample	N	Mean	StDev	SE Mean
Ler (Max)	5	0,00590	0,00504	0,00225
Lai (Max)	5	0,00746	0,00866	0,00387

Estimation for Paired Difference

Mean	StDev	SE Mean	95% CI for μ_difference
-0,00157	0,00841	0,00376	(-0,01200; 0,00887)

μ_difference: mean of (Ler (Max) - Lai (Max))

Test

Null hypothesis	H_0: μ_difference = 0
Alternative hypothesis	H_1: μ_difference ≠ 0

T-Value	P-Value
-0,42	0,698

Figure 3.22. *Maximal knee flexion/extension (left) and abduction/adduction (right) moments paired t-test comparison.*

Paired T-Test and CI: Ler (Min); Lai (Min)

Descriptive Statistics

Sample	N	Mean	StDev	SE Mean
Ler (Min)	5	-0,0625	0,0306	0,0137
Lai (Min)	5	-0,0670	0,0430	0,0192

Estimation for Paired Difference

Mean	StDev	SE Mean	95% CI for μ_difference
0,00454	0,02144	0,00959	(-0,02208; 0,03116)

μ_difference: mean of (Ler (Min) - Lai (Min))

Test

Null hypothesis	H_0: μ_difference = 0
Alternative hypothesis	H_1: μ_difference ≠ 0

T-Value	P-Value
0,47	0,660

Paired T-Test and CI: Ler (Min); Lai (Min)

Descriptive Statistics

Sample	N	Mean	StDev	SE Mean
Ler (Min)	5	-0,0386	0,0299	0,0134
Lai (Min)	5	-0,0444	0,0242	0,0108

Estimation for Paired Difference

Mean	StDev	SE Mean	95% CI for μ_difference
0,00577	0,00789	0,00353	(-0,00403; 0,01556)

μ_difference: mean of (Ler (Min) - Lai (Min))

Test

Null hypothesis	H_0: μ_difference = 0
Alternative hypothesis	H_1: μ_difference ≠ 0

T-Value	P-Value
1,63	0,177

Figure 3.23. *Minimal knee flexion/extension (left) and abduction/adduction (right) moments paired t-test comparison.*

3.4 Lerner and Lai-Arnold muscle forces during cycling

For the following graphs, forces are in Newton.

Results reported are for 2018Mar01-01, 2018Jan19-01, 2018Apr24-01, 2018Apr27-01 and 2018Jun08-01 participants averaged.

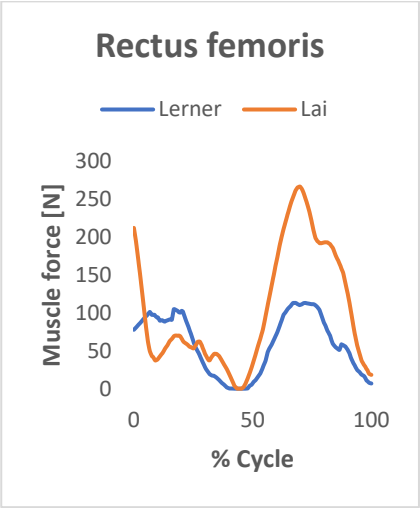

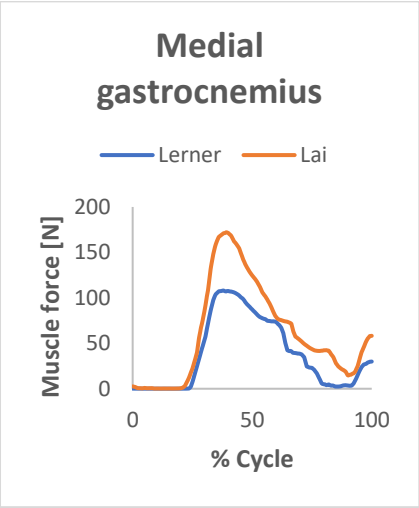

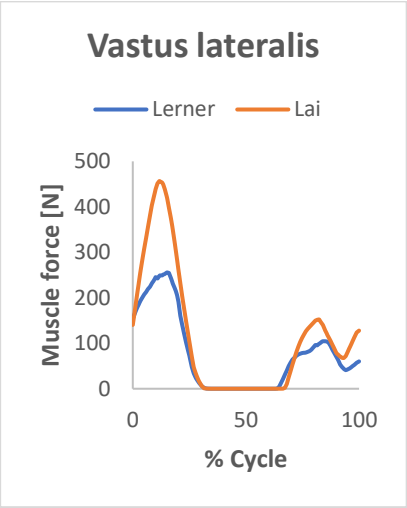

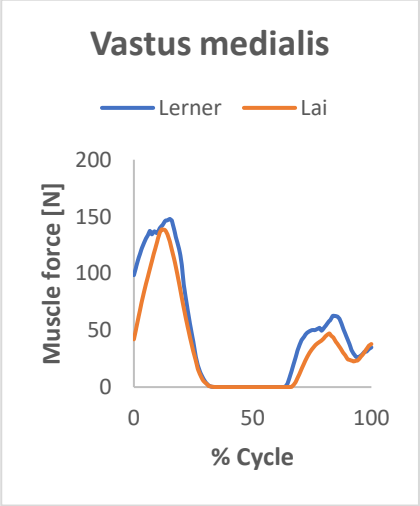

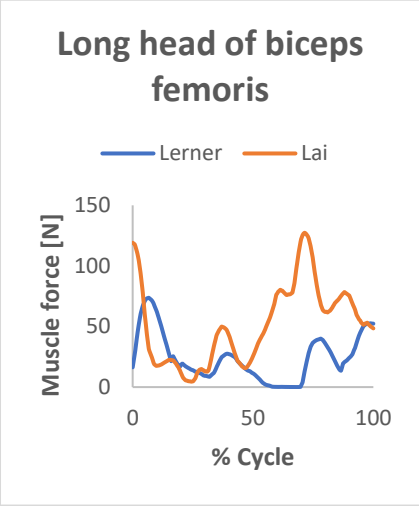

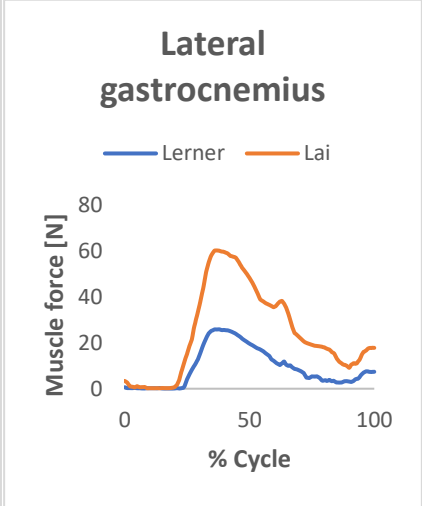

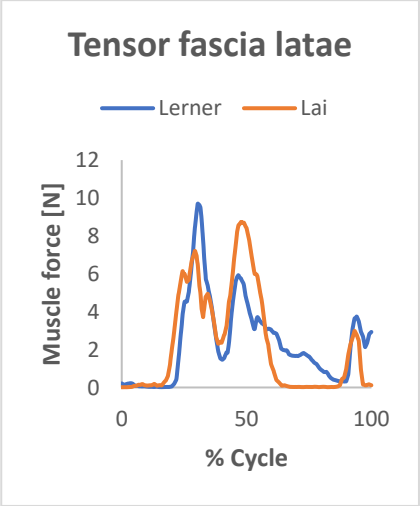

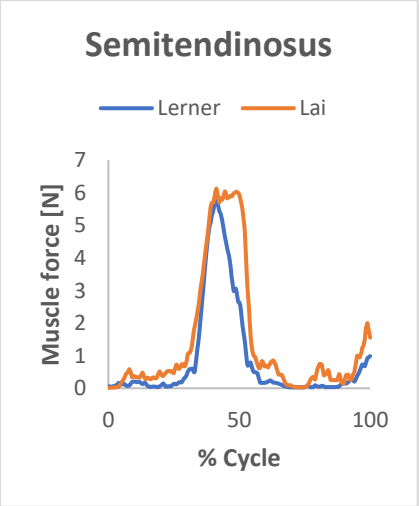

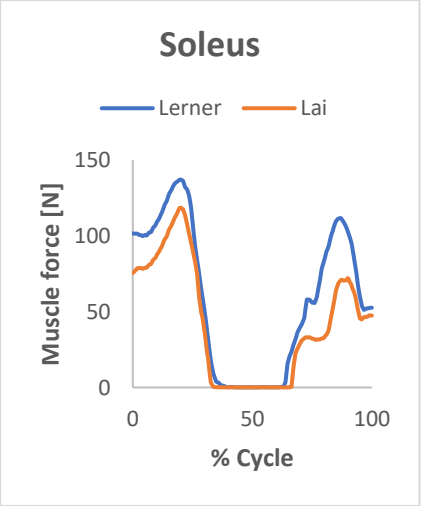

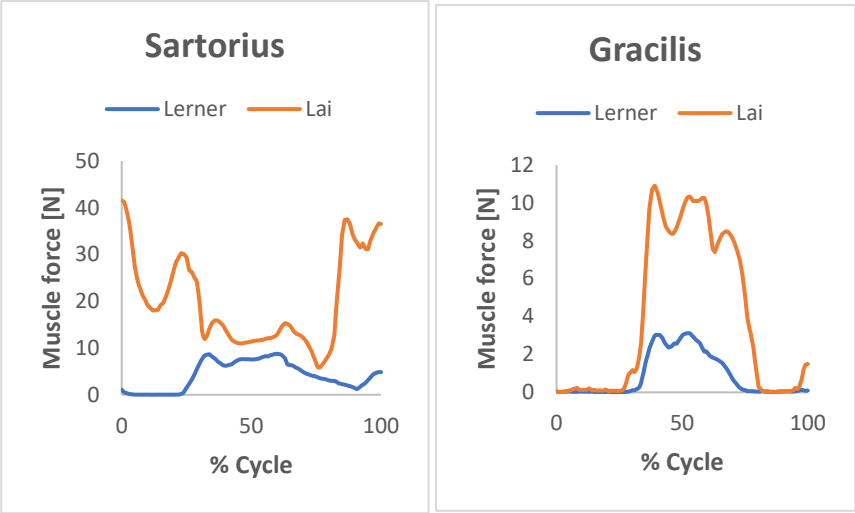

Figure 3.24: *Average muscle forces during cycling, computed with Lerner [17] and Lai [18] models.*

CHAPTER 4

DISCUSSION

The results from this study support the hypothesis that ML contact loads during cycling trials present a more equal distribution than during gait. The MLFR defined in the previous chapter is significantly different between gait and cycling when compared with its maximum, minimum and average value. Average MLFR for gait is around 4, this means that the medial compartment force is four times greater than the lateral one, confirming that [17] model is reliable in the prediction of the loads during gait [35].

Cycling has a MLFR average very close to 1, this means that TF loads during cycling are almost equally shared between the medial and the lateral compartment, matching the initial hypothesis. As drawback Lerner [17] shows significantly different TF loads during cycling with respect to Lai [18]. [18] predicts higher TF contact loads than [17], as a first explanation for this discrepancy has been thought that there could be a difference in FE and AA moments among the two models, but the statistical analysis shows that there isn't significant difference both for AA and FE moments predictions.

Another explanation could have been that the muscle parameters set in [18] could produce higher forces in the high articular flexion ranges, namely the flexion angles never reached by the participants during gait trials but that were reached during cycling.

Looking at FE and AA moments the highest moments are over 65% of the cycle, where FE moment becomes increasingly higher. The FE moment is also high at the beginning of the cycle, where the flexion angle is high, even if it could be compensated by the AA moment in which [17] predominates. It Can be stated that the only part of the cycle in which the moments are comparable is the central, comprised among 25% and 75% of the cycle, which is also the sole part in which the flexion angle is comparable with the one in gait.

The part in which the TF contact force differs the most is the beginning of the cycle (10-20%) which is around 100° flexion, followed by the contact force at 70 – 75% of the cycle, in which the flexion angle is still around 100°. 100° flexion represents an HF angle because, as already told in the previous section, the gait trials never cross 70° flexion, so this confirms the hypothesis that Lai predicts higher contact forces for HF angles.

Considering the muscles that contribute the most to TF contact forces can be stated that:

- For vastus lateralis Lai [18] predicts force almost two times higher than Lerner [17] at the beginning of the cycle (5-15% cycle). The maximal difference is around 250 N.
- For rectus femoris Lai [18] predicts force two times higher than Lerner [17] at the end of the cycle (65-75% cycle). Maximal difference around 160 N.
- For medial gastrocnemius Lai [18] predicts force approximately 1,5 higher than Lerner [17] in the central part of the cycle (35-45% cycle). Maximal difference around 60N.
- For long head biceps femoris Lai [18] predicts force 3 times higher than Lerner [17] at 65-75% cycle. Maximal difference around 80 N.

The largest muscle force that contributes during normal flexion angles (25-65%) is given by medial gastrocnemius, but it shows low force with respect to the muscles that contribute to the HF phases, therefore this could explain why the TF contact force difference between Lerner [17] and Lai [18] is higher during high flexion (0-25%/65-100%).
In the following table muscle parameters for both Lai [17] and Lerner [18] models have been reported:

	MAX ISOMETRIC FORCE [N]		**OPTIMAL FIBER LENGTH [CM]**		**TENDON SLACK LENGTH [CM]**		**PENNATION ANGLE [RAD]**	
	Ler	**Lai**	**Ler**	**Lai**	**Ler**	**Lai**	**Ler**	**Lai**
MEDIAL GASTROCNEMIUS	1558	3116	0.06	0.059	0.39	0.387	0.2967	0.1657
VASTUS LATERALIS	1871	5149	0.084	0.117	0.249	0.221	0.0873	0.2529
RECTUS FEMORIS	1169	2192	0.114	0.076	0.402	0.450	0.0872	0.2170
LATERAL GASTROCNEMIUS	683	1575	0.064	0.069	0.38	0.374	0.1396	0.2102
VASTUS MEDIALIS	1294	2748	0.089	0.11	0.22	0.208	0.0872	0.4222
LONG HEAD OF BICEPS FEMORIS	896	1313	0.109	0.098	0.326	0.333	0.0	0.1759
TENSOR FASCIAE LATAE	233	411.2	0.095	0.095	0.425	0.449	0.0524	0.0524
SEMITENDINOSUS	410	591.3	0.201	0.193	0.256	0.247	0.0873	0.2412
SARTORIUS	156	249.4	0.52	0.403	0.1	0.124	0.0	0.0261
GRACILIS	162	281.3	0.352	0.228	0.126	0.172	0.0524	0.1720

Table 4.1: *Muscle parameters for [17] and [18] models.*

CHAPTER 5

CONCLUSIONS

Lerner [17] shows an accurate medial and lateral TF loads partition, confirming the importance of improving this model in such a way that it could predicts accurately cycling medial and lateral TF loads as well. Indeed, Lerner [17] principal drawback is confirmed to be tibiofemoral loads prediction during cycling, which is significantly lower than what predicted by Lai [18], took as golden standard for this trial. To reach this goal is worth to work with vastus lateralis, rectus femoris and long head biceps femoris, trying to get the optimal parameters to solve the problem of their high force expression when the knee reaches HF angles.

Lerner [17] model shows a higher number of bodies representing the TF joint (femur, sagittal articulation frame, medial condyle, lateral condyle, tibial plateau, tibia, patella) with respect to Lai [18] (femur, tibia, patella). Furthermore, Lerner [17] shows a higher number of muscles, 92 in total, against the 80 muscles of Lai [18] model. This can suggest the possibility of merging the two models transferring Lai [18] principal characteristics in the compared model, in such a way to avoid the hard tasks of implementing new bodies and actuators that the opposite approach would imply. A drawback of this strategy could be the necessity of transferring the wrapping surfaces in Lerner [17], that have been introduced in Lai to improve the simulation speed. Future study goal should be to understand if these wrapping surfaces are crucial in the determination of TF contact loads, evaluating which is the best approach for merging the two models.

In the following table have been reported the main differences among Lerner [17] and Lai [18] models:

	PROS	CONS
LERNER [17]	• Accurate medial and lateral TF loads partition. • Bodies and muscles number closer to the physiological one with respect to Lai [18]. • Possibility to define TF alignment and ML compartment contact locations.	• Not accurate with tasks implying knee HF angles. • Doesn't show wrapping surfaces which could be computationally hard to transfer. • Knee flexion angle limited to the range: -120° - 10°.
LAI [18]	• Accurate TF contact load predictions with tasks implying knee HF angles. • Wrapping surfaces increase simulation speed. • Physiological knee flexion angle range.	• No ML load partition. • Show a lower number of bodies and muscles with respect to Lerner [17] which could be hard to transfer. • Not possible to define TF alignment and ML compartment contact locations

Table 4.2: *main differences among Lerner [17] and Lai [18] models*

REFERENCES

[1] Kutzner I, Heinlein B, Graichen F, et al. 2010. Loading of the knee joint during activities of daily living measured in vivo in five subjects. J Biomech 43:2164–2173

[2] Carter DR, Wong M. 1988. The role of mechanical loading histories in the development of diarthrodial joints. J Orthop Res 6:804–816.

[3] Baliunas A. 2002. Increased knee joint loads during walking are present in subjects with knee osteoarthritis. Osteoarthritis Cartilage 10:573–579.

[4] Schnitzer TJ, Popovich JM, Andersson GB, et al. 1993. Effect of piroxicam on gait in patients with osteoarthritis of the knee. Arthritis Rheum 36:1207–1213.

[5] Pottinger MV, Mavrommati K, Hazelwood SJ, Klisch SM. 2017. EMG61 Driven Inverse Dynamic Analysis of Knee Contact Forces During Gait and Cycling Using OpenSim. Biomechanics, Bioengineering, and Biotransport Conference.

[6] Heyde EA, Orekhov G, Robinson AM, Hazelwood SJ, and Klisch SM. 2018. Hip and knee forces for transtibial amputees in gait and cycling. 42nd Annual Meeting of the American Society of Biomechanics.

[7] Fregly BJ, Boninger ML. 2012. Personalized neuromusculoskeletal modeling to improve treatment of mobility impairments: A perspective from European research sites. Journal of NeuroEngineering and Rehabilitation. 9, 15, 3613 – 3621.

[8] Fregly BJ, Besier TF, Lloyd DG, et al. 2012. Grand challenge competition to predict in vivo knee loads. Journal of Orthopaedic Research 30, 4, 503–513.

[9] Ravera EP, Formento PAC, Crespo MJ, et al. 2011. Muscle-skeletal model of the thigh: a tool for understanding the biomechanics of gait in patients with cerebral palsy. Journal of Physics: Conference Series 332, 1, 012013.

[10] Delp SL, Anderson FC, Arnold AS, et Al. 2007. Opensim: opensource software to create and analyze dynamic simulations of movement. IEEE transactions on biomedical engineering 54, 11, 1940–1950.

[11] Saul KR, Hu X, Goehler CM, Vidt ME, et al. 2015. Benchmarking of dynamic simulation predictions in two software platforms using an upper limb musculoskeletal model. Computer Methods in Biomechanics and Biomedical Engineering 18, 13 1445–1458. PMID: 24995410.

[12] Delp SL, Loan JA. 1995. Graphics-based software system to develop and analyze models of musculoskeletal structures. Computers in Biology and Medicine 25, 1, 21 – 34.

[13] Dell'Isola A, Smith S, Andersen M, et al. 2017. Knee internal contact force in a varus malaligned phenotype in knee osteoarthritis (koa). Osteoarthritis and Cartilage.

[14] Jung Y, Koo Y, Koo S. Sep 2017. Simultaneous estimation of ground reaction force and knee contact force during walking and squatting. International Journal of Precision Engineering and Manufacturing 18, 9, 1263–1268.

[15] OpenSim. Opensim documentation. https://simtk-confluence.stanford.edu/display/OpenSim/Welcome+to+OpenSim. Accessed: 2019-06-10.

[16] DeMers MS, Pal S, Delp SL. 2014. Changes in tibiofemoral forces due to variations in muscle activity during walking. J. Orthop. Res.32, 769–776.

[17] Lerner ZF, DeMers MS, Delp SL, Browning RC. 2015. How tibiofemoral alignment and contact locations affect predictions of medial and lateral tibiofemoral contact forces. J Biomech 48:644-650.

[18] Lai AKM, Arnold AS, Wakeling JM. 2017. Why are Antagonist Muscles Co-activated in My Simulation? A Musculoskeletal Model for Analysing Human Locomotor Tasks. Annals of biomed eng., 45:2762-2774

[19] Rajagopal A, Dembia C, DeMers MS. 2016. Full body musculoskeletal model for muscledriven simulation of human gait. IEEE Trans. Biomed. Eng. 63:1–1.

[20] Liu MQ, Anderson FC, Schwartz MH, et al. 2008. Muscle contributions to support and progression over a range of walking speeds. J. Biomech. 41:3243–3252.

[21] Thelen DG, Anderson FC. 2006. Using computed muscle control to generate forward dynamic simulations of human walking from experimental data. J. Biomech. 39:1107–1115.

[22] Sharma L, Song J, Felson DT, et al. 2001.The role of knee alignment in disease progression and functional decline in knee osteoarthritis. J. Am. Med. Association 286, 188–195.

[23] Gerus P, Sartori M, Besier TF, et al. 2013. Subject-specific knee joint geometry improves predictions of medial tibiofemoral contact forces. J. Biomech. 46, 2778–2786.

[24] Halder A, Kutzner I, Graichen F, et al. 2012. Influence of limb alignment on mediolateral loading in total knee replacement: in vivo measurements in five patients. J. Bone Joint Surg. 94,1023–1029.

[25] Kutzner I, Bender A, Dymke J, et al. 2017. Mediolateral force distribution at the knee joint shifts across activities and is driven by tibiofemoral alignment. Bone Joint J. 99-B:779–87.

[26] Zhao D, Banks SA, Lima DD, et al. 2007. In vivo medial and lateral tibial loads during dynamic and high flexion Activities. Wiley Periodicals, Inc. J Orthop Res 25:593–602.

[27] Amti. Netforce user manual. Amti (Watertown, Ma, Usa), version 3.05.01, 2010.

[28] Amti. Accugait installation guide and manual, version 1.6. amti (Watertown, Ma, Usa), Feb 2007.

[29] Amti. Ad 2.5d sensor data sheet. Amti (Watertown, Ma, Usa), Jan 2013.

[30] Amti. Ad 2.5d sensor manual. Amti (Watertown, Ma, Usa), Jan 2013.

[31] Amti. Gen5 user manual and programmers reference. version 1.2 Amti (Watertown, Ma, Usa), Feb 2012.

[32] Matlab. Matlab documentation. http://it.mathworks.com/help/matlab/. Accessed: 2017-09-05.

[33] OpenSim. OpenSim documentation. https://simtk-confluence.stanford.edu/display/OpenSim/Welcome+to+OpenSim. Accessed: 2019-06-25.

[34] Vtk. Vtk website. https://www.vtk.org. Accessed: 2019-06-26.

[35] Johnson F, Leitl S, Waugh W. 1980. The distribution of load across the knee, a comparison of static and dynamic measurements. Journal of bone and joint surgery.

[36] Thelen DG. 2003. Adjustment of muscle mechanics model parameters to simulate dynamic contractions in older adults. ASME Journal of Biomechanical Engineering. 125(1):70–77.

[37] Millard M, Uchida T, Seth A, et al. 2013. Flexing computational muscle: modeling and simulation of musculotendon dynamics. ASME Journal of Biomechanical Engineering. 135(2):021005.

[38] OpenSim. OpenSim documentation. https://simtk-confluence.stanford.edu:8443/display/OpenSim/OpenSim+Models. Accessed: 2019-09-09.

[39] Van Melick N, Meddeler BM, Hoogeboom TJ, et al. 2017. How to determine leg dominance: The agreement between self-reported and observed performance in healthy adults. PLoS ONE. 12(12): e0189876.

[40] Damm P, Kutzner I, Bergmann G, et a. 2017. Comparison of in vivo measured loads in knee, hip and spinal implants during level walking. Journal of Biomechanics, 51, 128–132. doi:10.1016/j.jbiomech.

[41] Kutzner I, Heinlein B, Graichen F, et al. 2012. Loading of the Knee Joint During Ergometer Cycling: Telemetric In Vivo Data. Journal of Orthopaedic & Sports Physical Therapy. 42(12), 1032–1038. doi:10.2519/jospt.2012.4001

APPENDIX A

LAI-ARNOLD AND LERNER MODELS MERGING ATTEMPTS

The model used to perform all the following analysis is 'uninformed', this means that the generic frontal-plane locations of the medial/lateral compartment structures are 20mm medial and lateral of the knee joint center. The tibiofemoral alignment for this model in 180 deg.

A.1 10 muscles model

The changes attached to Lerner model to obtain the current model are:

- Location, Pennation angle, fiber length and tendon slack length for the following 10 muscles: semitendinosus (semiten), long head of the biceps femoris (bifemlh), sartorius (sar), rectus femoris (recfem), tensor fascia latae (tfl), gracilis (grac), vastus medialis (vasmed), vastus lateralis (vaslat), and medial (medgas) and lateral (latgas) gastrocnemii.

The reason why these models shows only 10 muscles is that in the other merging attempts (reported in section A.4) the hip muscles were causing contact forces way too high in gait.
The drawback of this model is that during gait the force expressed by medial gastrocnemius (MG), derived from static optimization, is too low. This can be the explanation for such low tibial contact force in the second peak of gait, around 50% of the trial.

A.1.1 GAIT RESULTS

For the following graphs, forces are in Newton, '[%] Cycle' is normalized time from first heel strike (0%) to next heel strike (100%). The zero value of the knee flexion range is intended as the fully extended knee. Results are computed and averaged over 3 full cycles for 2018Mar01-01 and 2018Jan19-01 participants.

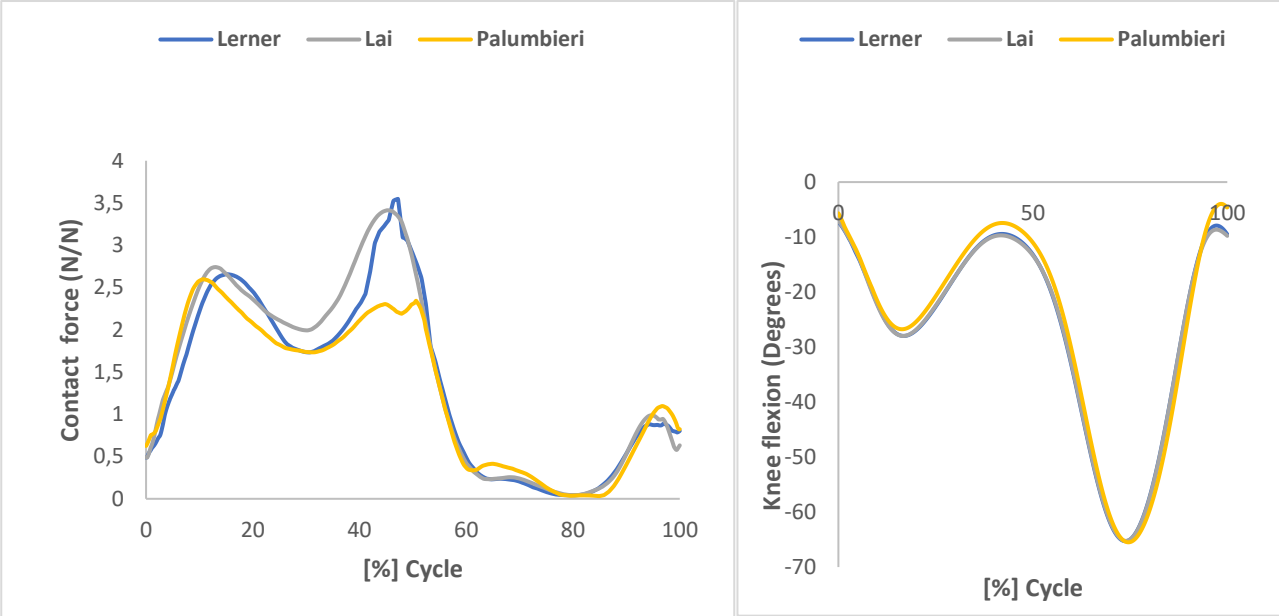

Figure A.1: *Total tibial contact forces (left) and knee flexion angles (right) computed with Lerner, Lai-Arnold and 10 muscles (Palumbieri) models averaging data from 2018Mar01-01 and 2018Jan19-01 participants.*

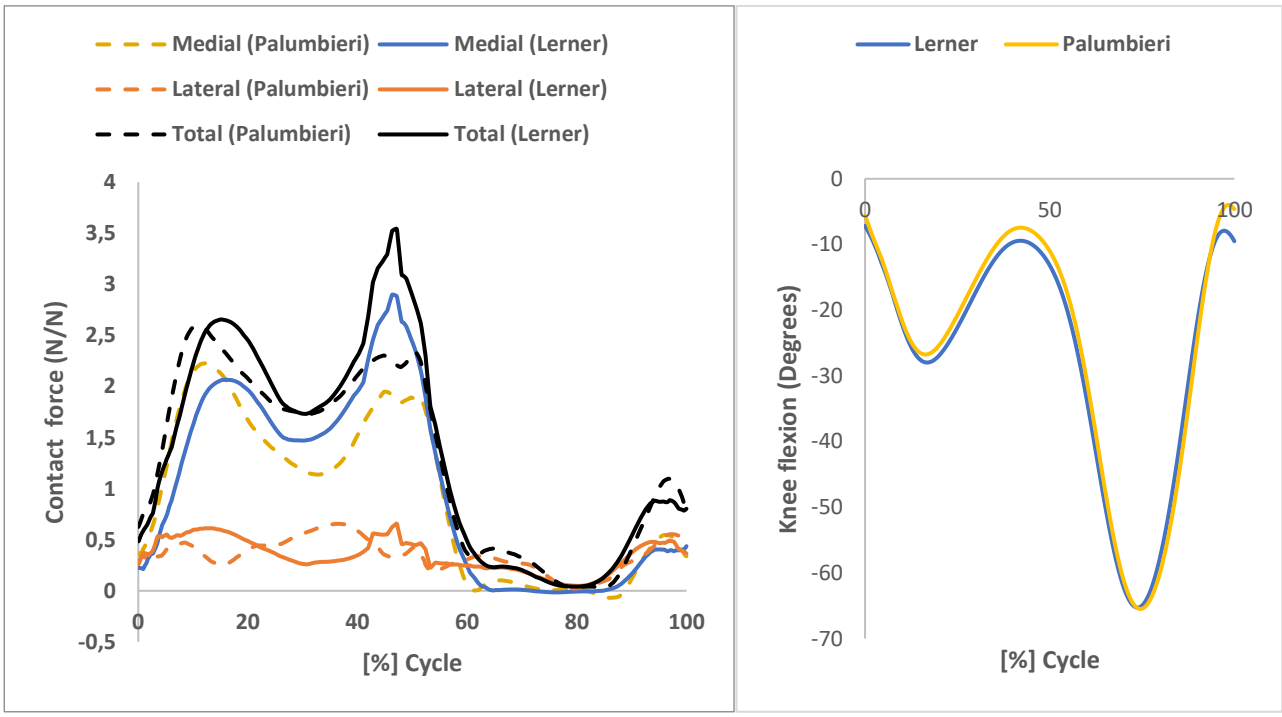

Figure A.2: *Tibial contact forces (left) and knee flexion angles (right) computed with 10 muscles (here reported as Palumbieri) model (dashed lines) and Lerner model (solid line) averaging data from 2018Mar01-01 and 2018Jan19-01 participants.* *a.1.2*

A.1.2 CYCLING RESULTS

For the following graphs, forces are in Newton, '[%] Cycle' is normalized time from the first top dead center (0%) to second top dead center (100%). The zero value of the knee flexion range is intended as the fully extended knee. Results are computed and averaged over 3 full cycles for 2018Mar01-01 and 2018Jan19-01 participants.

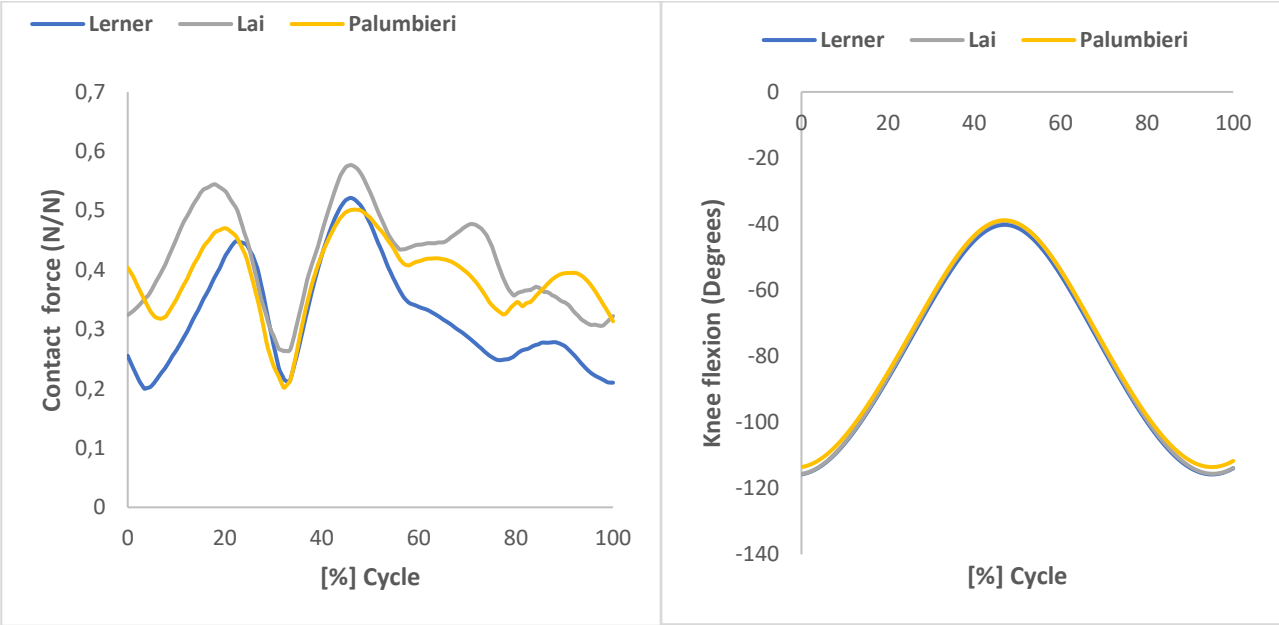

Figure A.3: *Total tibial contact forces (left) and knee flexion angles (right) computed with Lerner, Lai-Arnold and 10 muscles (Palumbieri) models averaging data from 2018Mar01-01 and 2018Jan19-01 participants.*

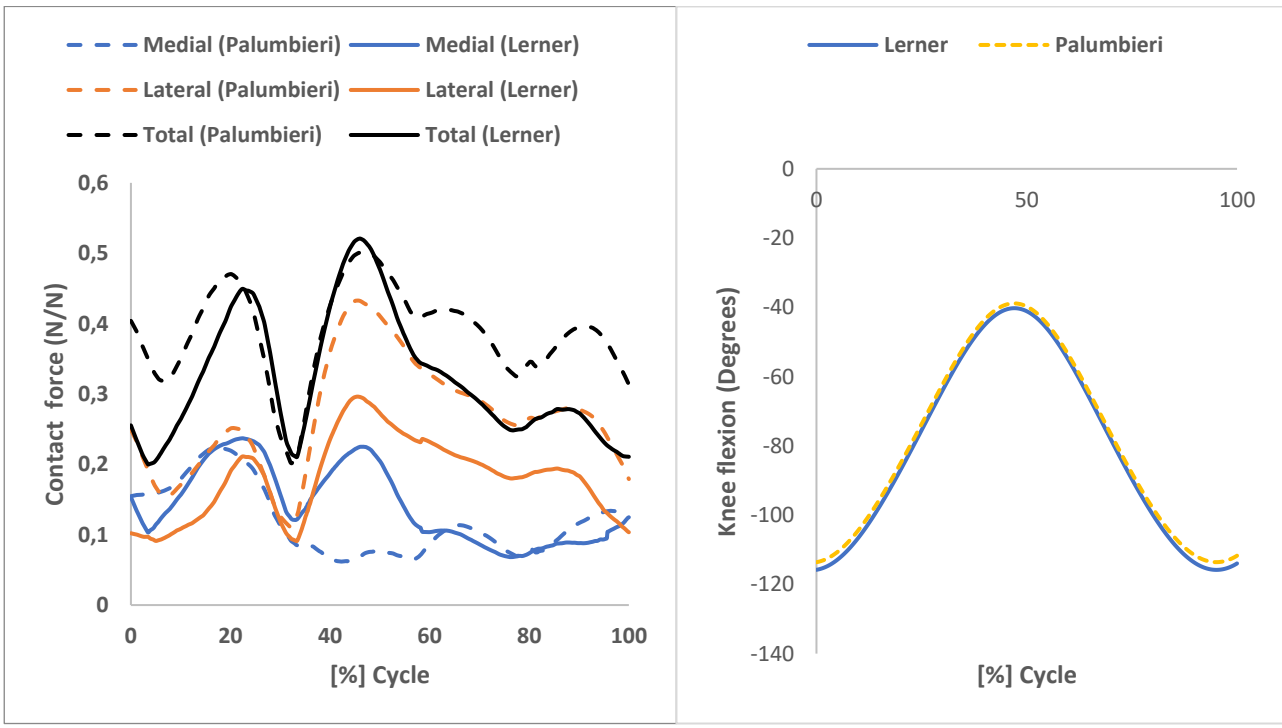

Figure A.4: *Tibial contact forces (left) and knee flexion angles (right) computed with 10 muscles (Palumbieri) model (dashed lines) and Lerner model (solid line) averaging data from 2018Mar01-01 and 2018Jan19-01 participants.*

A.2 9 muscles model

The changes attached to Lerner model to obtain the current model are:

- Isometric force, location, pennation angle, fiber length and tendon slack length for the following 9 muscles: semitendinosus (semiten), long head of the biceps femoris (bifemlh), sartorius (sar), rectus femoris (recfem), tensor fascia latae (tfl), gracilis (grac), vastus medialis (vasmed), vastus lateralis (vaslat) and lateral (latgas) gastrocnemius.

This model shows one updated muscle less with respect to the previous, medial gastrocnemius is left unmodified because the force expressed during gait was too low when updated with Lai-Arnold model parameters. As results can be said that cycling tibial contact forces are reasonable but the second peak of gait is still too low.

A.2.1 GAIT RESULTS

For the following graphs, forces are in Newton, '[%] Cycle' is normalized time from first heel strike (0%) to next heel strike (100%). The zero value of the knee flexion range is intended as the fully extended knee. Results are computed and averaged over 3 full cycles for 2018Mar01-01 and 2018Jan19-01 participants.

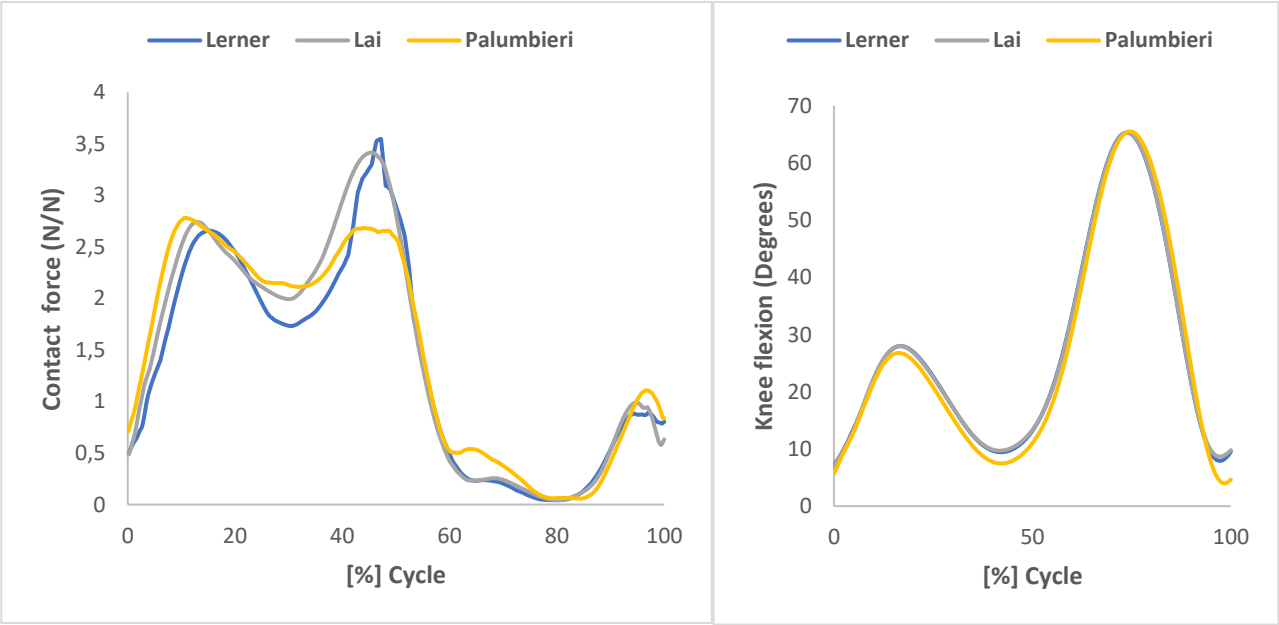

Figure A.5: *Total tibial contact forces (left) and knee flexion angles (right) computed with Lerner, Lai-Arnold and 9 muscles (Palumbieri) models averaging data from 2018Mar01-01 and 2018Jan19-01 participants.*

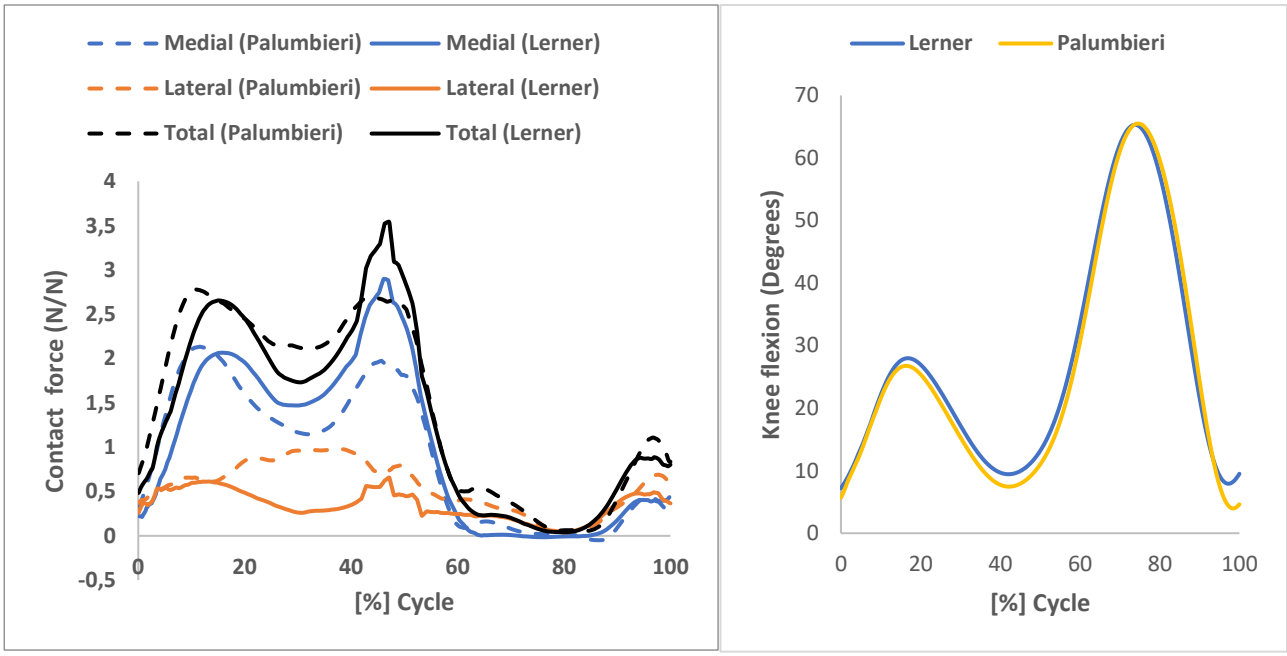

Figure A.4: Tibial contact forces (left) and knee flexion angles (right) computed with 9 muscles (here reported as Palumbieri) model (dashed lines) and Lerner model (solid line) averaging data from 2018Mar01-01 and 2018Jan19-01 participants.

A.2.2 CYCLING RESULTS

For the following graphs, forces are in Newton, '[%] Cycle' is normalized time from the first top dead center (0%) to second top dead center (100%). The zero value of the knee flexion range is intended as the fully extended knee. Results are computed and averaged over 3 full cycles for 2018Mar01-01 and 2018Jan19-01 participants.

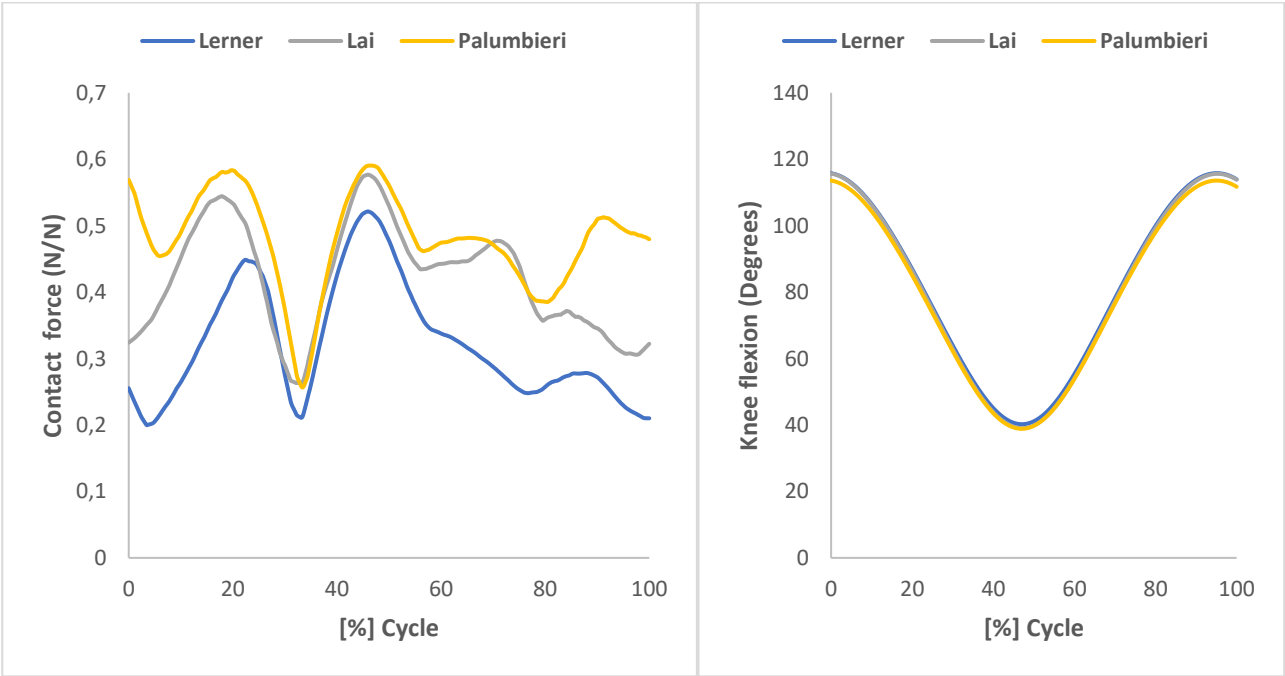

Figure A.7: Total tibial contact forces (left) and knee flexion angles (right) computed with Lerner, Lai-Arnold and 9 muscles (Palumbieri) models averaging data from 2018Mar01-01 and 2018Jan19-01 participants.

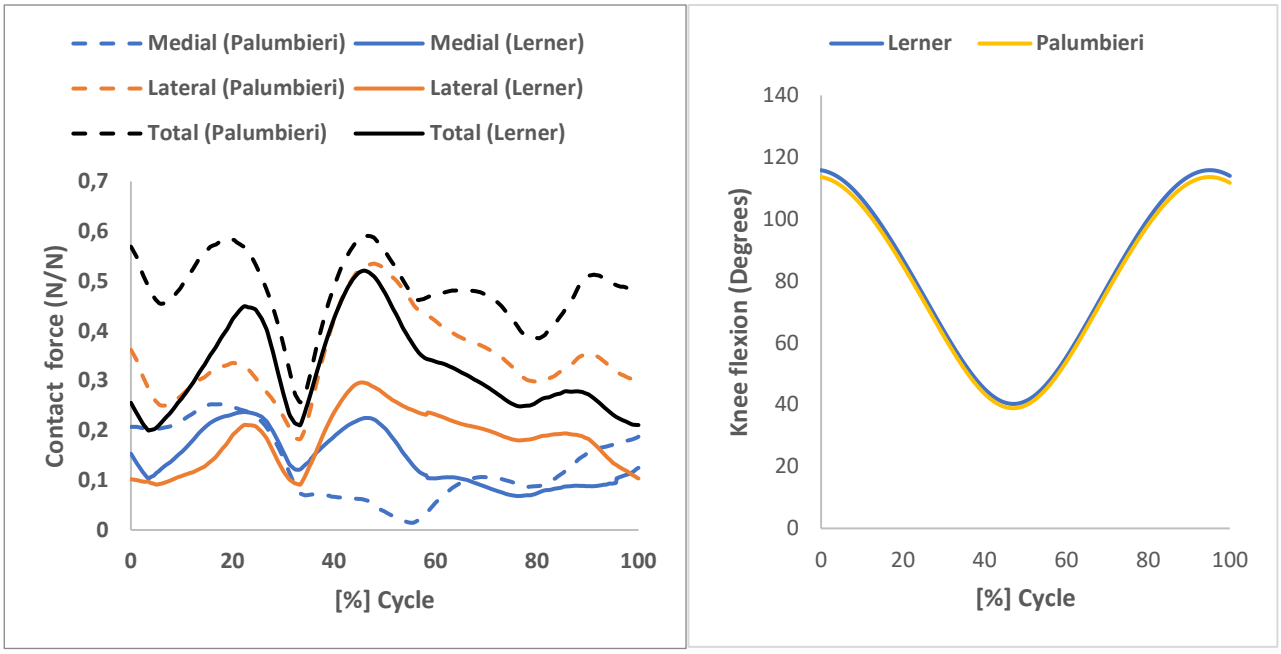

Figure A.8: *Tibial contact forces (left) and knee flexion angles (right) computed with 9 muscles (here reported as Palumbieri) model (dashed lines) and Lerner model (solid line) averaging data from 2018Mar01-01 and 2018Jan19-01 participants.*

A.3 Isometric 10 muscles model

Isometric force, location, pennation angle, fiber length and tendon slack length for the following 10 muscles: semitendinosus (semiten), long head of the biceps femoris (bifemlh), sartorius (sar), rectus femoris (recfem), tensor fascia latae (tfl), gracilis (grac), vastus medialis (vasmed), vastus lateralis (vaslat), and medial (medgas) and lateral (latgas) gastrocnemii.

A.3.1 GAIT RESULTS

For the following graphs, forces are in Newton, '[%] Cycle' is normalized time from first heel strike (0%) to next heel strike (100%). The zero value of the knee flexion range is intended as the fully extended knee. Results are computed and averaged over 3 full cycles for 2018Mar01-01 and 2018Jan19-01 participants.

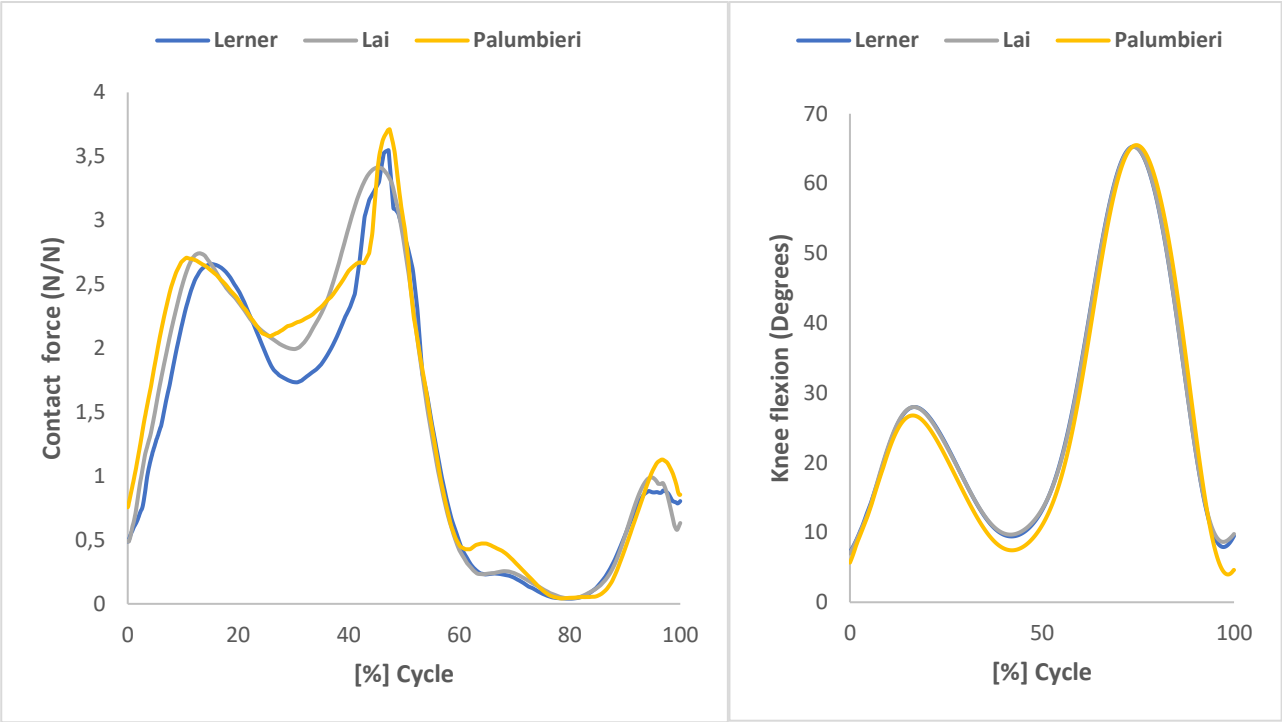

Figure A.9: *Total tibial contact forces (left) and knee flexion angles (right) computed with Lerner, Lai-Arnold and Isometric 10M (Palumbieri) models averaging data from 2018Mar01-01 and 2018Jan19-01 participants.*

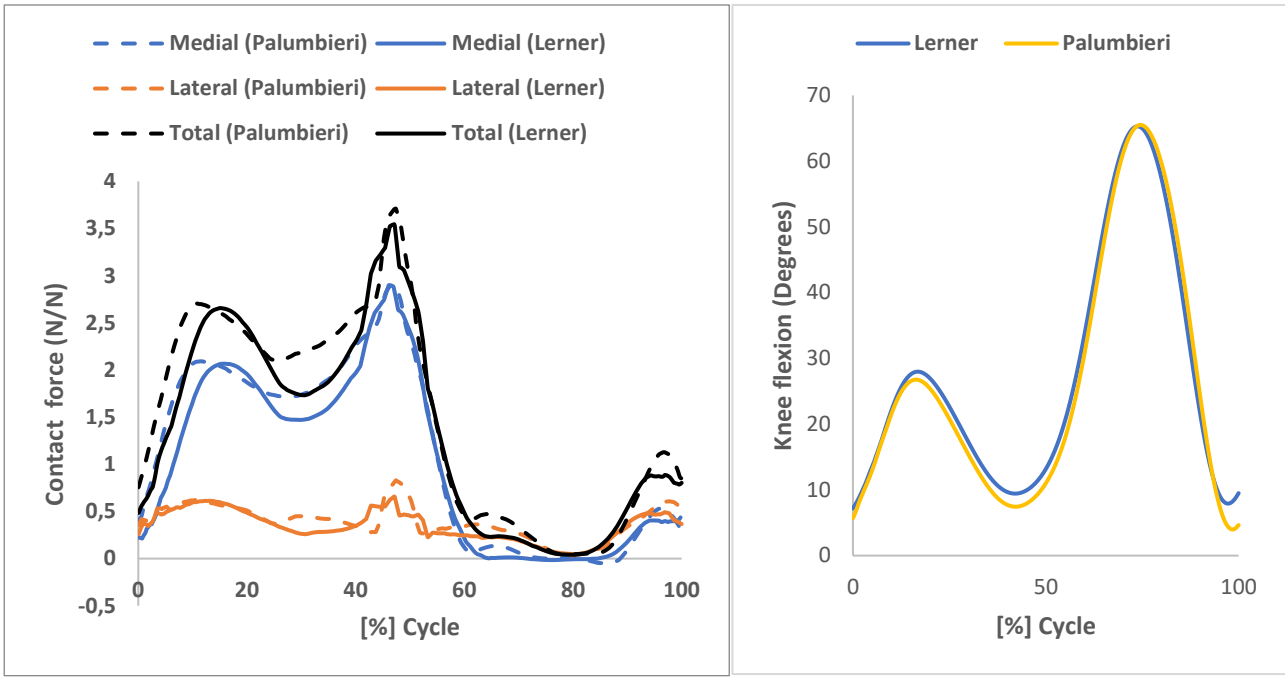

Figure A.10: *Tibial contact forces (left) and knee flexion angles (right) computed with Isometric 10M (here reported as Palumbieri) model (dashed lines) and Lerner model (solid line) averaging data from 2018Mar01-01 and 2018Jan19-01 participants.*

A.3.2 CYCLING RESULTS

For the following graphs, forces are in Newton, '[%] Cycle' is normalized time from the first top dead center (0%) to second top dead center (100%). The zero value of the knee flexion range is intended as the fully extended knee. Results are computed and averaged over 3 full cycles for 2018Mar01-01 and 2018Jan19-01 participants.

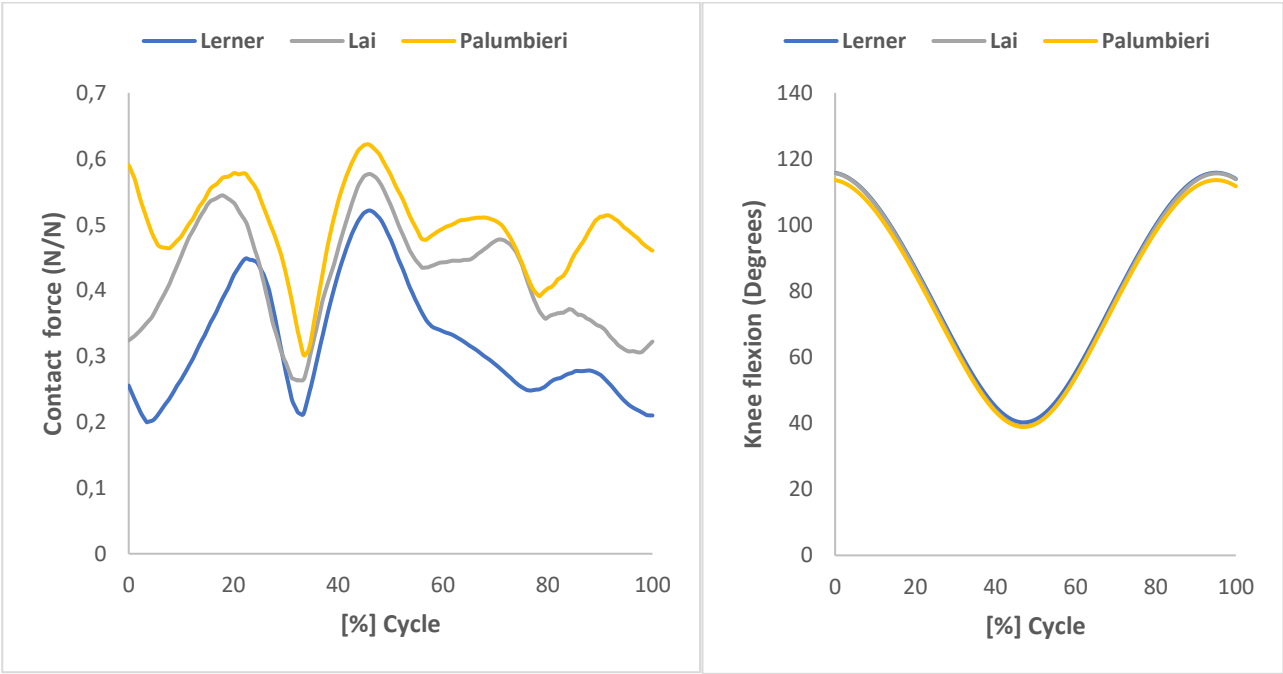

Figure A.11: *Total tibial contact forces (left) and knee flexion angles (right) computed with Lerner, Lai-Arnold and Isometric 10M (Palumbieri) models averaging data from 2018Mar01-01 and 2018Jan19-01 participants.*

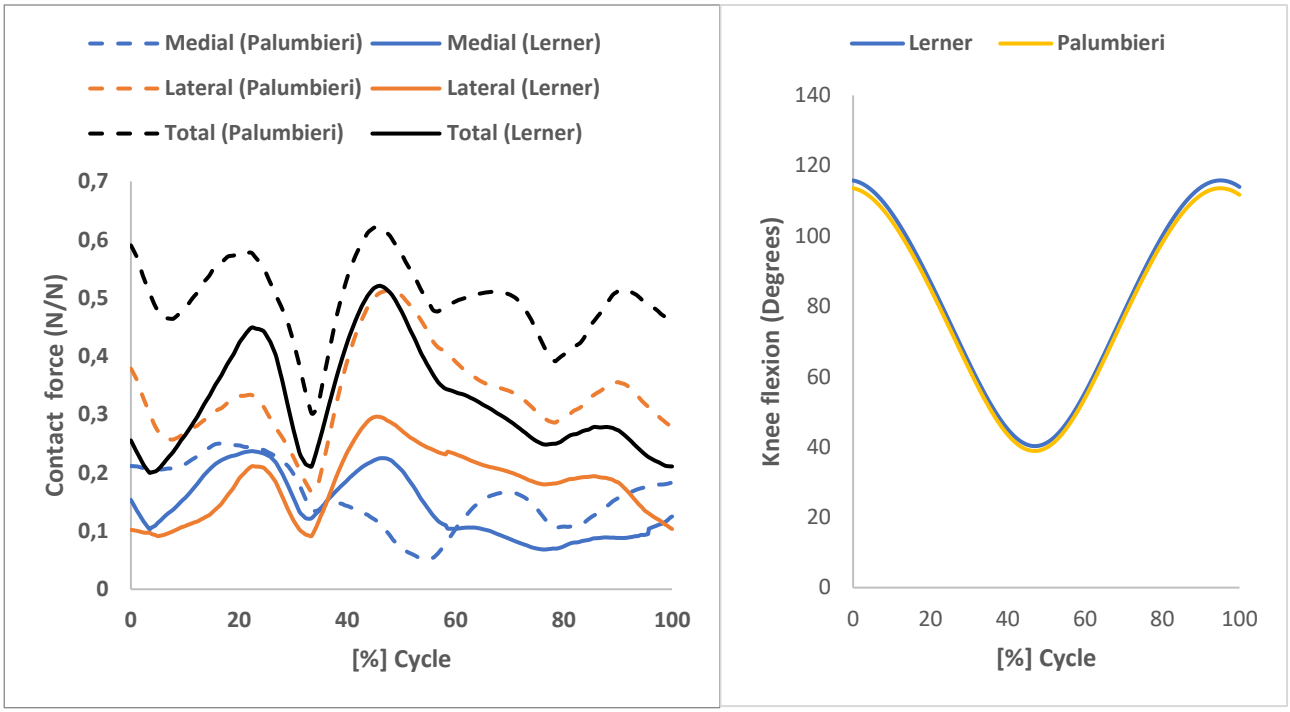

Figure A.12: *Tibial contact forces (left) and knee flexion angles (right) computed with Isometric 10M (here reported as Palumbieri) model (dashed lines) and Lerner model (solid line) averaging data from 2018Mar01-01 and 2018Jan19-01 participants.*

A.4 OTHER UPDATES

Here follow the updates attached to Lerner model:

NAME	MODIFIED MUSCLES	MODIFIED PARAMETERS	COMMENTS
Body	No one	Addition of tibial wrapping surfaces	For cycling results, the model looks more similar to Lerner than Lai, even if the expectation would be the opposite.
Muscle	Everyone, less than Add_mag_isch, gas_lat, gas_med, bifemsh	Increase the knee flexion range from 120 degrees to 140. Modify optimal fiber length, tendon slack length, pennation angles and attachment location.	The muscles that weren't modified were left unchanged because they were the only ones that, while updating attachment location, required a change of body attachment. The Results are strongly distorted.
Fiber Length 10M	10M	Fiber Length	Compared to Lerner: increases MG force. Increases Tensor fasciae Latae (TFL) force a lot. Increases Rectus Femoris force a bit at the first peak for gait. Compared to Lai-Arnold: Increases Biceps Femoris (BF) force a little.
Location 10M	10M	Attachment location	Compared to Lerner: increases TFL force a lot, also increases RF first peak. Compared to Lai-Arnold: Increases TFL force a lot, decrease MG force a lot.
Pennation 10M	10M	Pennation angle	Compared to Lerner: increases TFL and MG force a lot, with TFL magnitudes a bit lower than MG ones). Increases RF a lot at the first peak. Compared to Lai-Arnold:

			Increases MG force a lot. Increases RF force at the first peak.
Slack length 10M	10M	Tendon slack length	Compared to Lerner: Increases MG force a lot, also substantial increases are for RF, BF and TFL. Compared to Lai-Arnold: Increases TFL and BF forces a lot.
IsoCtrl 10M	10M	Fiber length, attachment location, pennation angle, tendon slack length, isometric force, minimal control force	With respect to the Isometric 10M model: Distorts a lot total TF contact force for gait, decreasing strongly the second peak. TF contact force raises a lot during cycling.
Isometric 9M	9M	Fiber length, attachment location, pennation angle, tendon slack length, isometric force	Decreases a lot the second peak during gait.
Omnia	All	Isometric force, Location, pennation angle, fiber length and tendon slack length for all the muscles that find a correspondence in Lai-Arnold model.	Distorts a lot the gait results. TF contact force during cycling is highly increased.
Parameters	All	Isometric force, Pennation angle, fiber length and tendon slack length for all the muscles that find a correspondence in Lai-Arnold model.	Distorts gait results a lot. Similar to Lai during cycling when 50% of the task is crossed.

Table A.1: *Other Lerner [17] - Lai [18] merging attempts.*

N.B. As 10M are intended the following muscles: semitendinosus (semiten), long head of the biceps femoris (bifemlh), sartorius (sar), rectus femoris (recfem), tensor fascia latae (tfl), gracilis (grac), vastus medialis (vasmed), vastus lateralis (vaslat), and medial (medgas) and lateral (latgas) gastrocnemii.

As 9M are intended the muscles reported as in 10M description less than medial gastrocnemius.

Other updates that have been attempted are:

- Add tibia, femur and pelvis wrapping surfaces: the model worked only with the tibial wrapping surfaces, it was impossible to add femur and pelvis wrapping surfaces. This is probably because the wrapping surfaces are related to the muscle model determining the force and producing properties of each muscle. The muscles properties in [17] have been defined following the 'Thelen muscle model' [36], while the properties in [18] have been defined according to the 'Millard muscle model' [37]. Resolving this problem will probably require a deeper comprehension of ANSI C++ coding.
- Add patellofemoral constraints: the model gave problems while performing RRA with knees rotating in non-physiological directions. In this case, the constraint is related to a coordinate named 'Knee_angle_beta' in Lai-Arnold model, which doesn't exist in Lerner.

In the future could be worth to try to add the aforementioned wrapping surfaces, unfortunately, this shouldn't be a trivial work. An option to simplify this problem could be to reverse the approach on how these two models have been tried to be merged. This study has been attempted to modify Lerner model adding the particular features of Lai model, this has been done because Lerner shows a major number of bodies and muscles with respect to Lai, which could be problematic to transfer. An important work for the next study will be to understand if is simpler to transfer these muscles and body in Lerner model or fitting the wrapping surfaces on Lai.